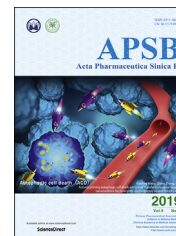




Chinese Pharmaceutical Association  
Institute of Materia Medica, Chinese Academy of Medical Sciences

Acta Pharmaceutica Sinica B

[www.elsevier.com/locate/apsb](http://www.elsevier.com/locate/apsb)  
[www.sciencedirect.com](http://www.sciencedirect.com)



REVIEW

# Multifunctional oral delivery systems for enhanced bioavailability of therapeutic peptides/proteins



Ying Han<sup>a</sup>, Zhonggao Gao<sup>a,\*</sup>, Liqing Chen<sup>a</sup>, Lin Kang<sup>a</sup>, Wei Huang<sup>a</sup>, Mingji Jin<sup>a</sup>, Qiming Wang<sup>a</sup>, You Han Bae<sup>b</sup>

<sup>a</sup>State Key Laboratory of Bioactive Substance and Function of Natural Medicines, Department of Pharmaceutics, Institute of Materia Medica, Chinese Academy of Medical Sciences and Peking Union Medical College, Beijing 100050, China

<sup>b</sup>Department of Pharmaceutics and Pharmaceutical Chemistry, the University of Utah, Salt Lake City, UT 84108, USA

Received 18 September 2018; received in revised form 28 October 2018; accepted 28 November 2018

## KEY WORDS

Multifunctional delivery systems;  
Oral;  
Bioavailability;  
Macromolecules;  
Peptides and proteins;  
Gastrointestinal environment;  
Epithelial barriers;  
Nanoparticles

**Abstract** In last few years, therapeutic peptides/proteins are rapidly growing in drug market considering their higher efficiency and lower toxicity than chemical drugs. However, the administration of therapeutic peptides/proteins is mainly limited in parenteral approach. Oral therapy which was hampered by harsh gastrointestinal environment and poorly penetrating epithelial barriers often results in low bioavailability (less than 1%–2%). Therefore, delivery systems that are rationally designed to overcome these challenges in gastrointestinal tract and ameliorate the oral bioavailability of therapeutic peptides/proteins are seriously promising. In this review, we summarized various multifunctional delivery systems, including lipid-based particles, polysaccharide-based particles, inorganic particles, and synthetic multifunctional particles that achieved effective oral delivery of therapeutic peptides/proteins.

© 2019 Chinese Pharmaceutical Association and Institute of Materia Medica, Chinese Academy of Medical Sciences. Production and hosting by Elsevier B.V. This is an open access article under the CC BY-NC-ND license (<http://creativecommons.org/licenses/by-nc-nd/4.0/>).

\*Corresponding author. Tel./fax +86 10 6302 8096.

E-mail address: [zgao@imm.ac.cn](mailto:zgao@imm.ac.cn) (Zhonggao Gao).

Peer review under responsibility of Institute of Materia Medica, Chinese Academy of Medical Sciences and Chinese Pharmaceutical Association.

## 1. Introduction

Therapeutic peptides/proteins presenting superior potencies and fewer side effects compared to chemical drugs are springing up like mushrooms in drug market recently. With the common physicochemical characteristics of high molecular weight (MW), hydrophilicity and enzyme/pH sensitivity, protein drugs presenting poor oral bioavailability are almost administered parenterally, while only few of them, for instance, desmopressin, glutathione, etc., are commercially available<sup>1</sup>. The development of oral administration for peptides/proteins as a non-invasive therapeutic method has emerged as an attractive alternate to the parenteral route in recent years, considering long-term dosing, safety, convenience, less pain and fewer burdens of medical costs<sup>2</sup>. It is the most advantageous approach of drug delivery, in particular for the treatment of chronic diseases such as diabetes and hepatitis B, which demand long-term drug administration. Especially, the pharmacokinetics (PK) of insulin (Ins) delivered orally mimics the pulsatile secretion pattern and physiological fate of endogenous Ins in the body, which is delivered to the liver exploiting the first-pass metabolism rather than peripheral tissues leading to a lot side effects compared with parenteral administration<sup>3</sup>. Moreover, in paediatric use, human growth hormone (hGH) has to be given per day during a long time, which makes the parenteral administration unacceptable, particularly when applying to younger children. Several efforts have been made in recent years for oral delivery of therapeutic peptides/proteins. Part of promising oral delivery systems of peptides/proteins have progressed to clinical trials, as indicated in Table 1. However, peptides/proteins usually have poor oral bioavailability (<2%) due to the unfavorable physiological environment (pH, enzymes) and complex biological barriers (mucus layer, epithelial cells, tight junctions) in the gastrointestinal tract (GIT)<sup>4</sup> (Fig. 1). To overcome the harsh environments in GIT for oral delivery of therapeutic peptides/proteins and improve their oral bioavailability, increasing number of multifunction systems are designed and researched. Summary of representative therapeutic peptides/proteins under research for oral delivery are listed in Table 2.

### 1.1. Gastrointestinal barriers

Multiple digestive enzymes such as pepsin, chymotrypsin, trypsin and bile salts in the GIT may lead to early leakage and degradation of the cargos. Besides, complex pH values varying in different regions of the GIT intensified the difficulties of oral delivery as pH 2.0–4.0 in stomach, pH ~5.5 in duodenum, pH ~6.0 in jejunum,

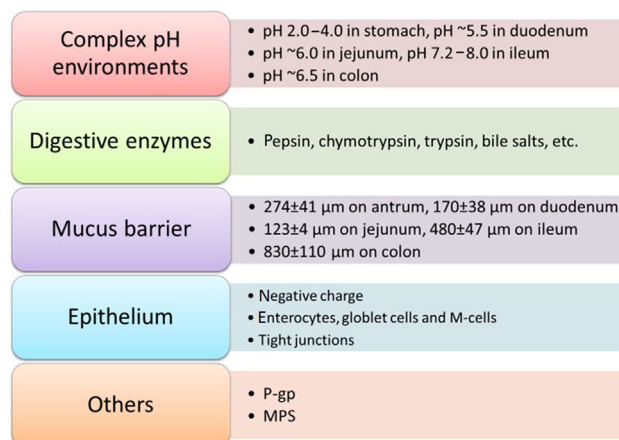


**Figure 1** The physiological barriers during oral absorption of peptides/proteins.

pH 7.2–8.0 in ileum and pH ~6.5 in colon<sup>56</sup>. Even if these challenges above are safely undergone, the mucosal layer covering the entire GIT, which lubricates and protects the epithelial layer, would keep out most foreign particles. The mean thicknesses of mucus in different regions of the GIT alter greatly by  $274 \pm 41 \mu\text{m}$  on antrum,  $170 \pm 38 \mu\text{m}$  on duodenum,  $123 \pm 4 \mu\text{m}$  on jejunum,  $480 \pm 47 \mu\text{m}$  on ileum and  $830 \pm 110 \mu\text{m}$  on colon<sup>57</sup>. In addition, the glycosylation of threonine, proline and serine domains in mucins endow the epithelium with negative charge. The intestinal epithelium mainly composed of three kinds of cells: enterocytes, goblet cells and Microfold cells (M-cells), in which enterocytes are the majority, goblet cells that secrete mucin occupied 10%–20% of epithelial cells, M-cells mainly located in Peyer's patches in the ileum representing less than 1% of the total epithelial surface are capable of transporting drugs from the epithelium to the underlying lymphoid tissues<sup>58</sup>. Tight junctions (TJs) localized between the intestinal epithelial cells are another restrictions towards the absorption of hydrophilic peptides/proteins *via* paracellular way, of which the gap is about 7–9 Å for the jejunum, 3–4 Å for the ileum, and 8–9 Å for the colon<sup>59</sup>.

### 1.2. Strategies to overcome the barriers in GIT

To safely pass the gastric acid in stomach, enteric materials have been applied to encapsulate drug carriers to make them more resistant to the environment as well as control their release<sup>60</sup>. However, the enteric polymer coated may not dissolve completely in the small

**Table 1** Examples of clinically delivery systems for oral peptides/proteins (clinicaltrials.gov).

Technology	Drug	Phase	Company
Eligen <sup>®</sup>	Insulin	I	Emisphere Technologies, Inc. (USA)
Mycopssa <sup>™</sup>	Octreotide	III	Chiasma, Inc. (USA)
Peptelligence <sup>™</sup>	Leuprolide	II	Enteris BioPharma, Inc. (USA)
Eligen <sup>®</sup>	GLP-1	II	University Hospital, Basel (Switzerland)
Peptelligence <sup>™</sup>	PTH	II	Entera Bio Ltd. (Israel)
Eligen <sup>®</sup>	Semaglutide	III	Novo Nordisk A/S (Denmark)
Eligen <sup>®</sup>	Salmon calcitonin	III	Nordic Bioscience A/S (Denmark) and Novartis (Switzerland)
POD <sup>™</sup>	Insulin	II	Oramed, Ltd. (Israel)
Oshadi Icp	Insulin	I	Oshadi Drug Administration (Israel)
Peptelligence <sup>™</sup>	Salmon calcitonin	II	Tarsa Therapeutics, Inc. (USA)

**Table 2** Representative therapeutic peptides/proteins under research for oral delivery.

Name	Structure/composition	Primary therapy	Ref.
EGFR targeted hybrid peptide	In a total of 32 amino acid residues and a molecular weight of 3774 Da	Highly selective activity toward EGFR-positive cancer cells	5
Vancomycin	A branched tricyclic glycopeptide	Infections by Gram-positive bacteria	6
Myrcludex B	A linear myristoylated peptide composed of 47 amino acids	Hepatitis B	7
hGH	A 191 amino acids protein	Adult growth hormone deficiency and children's growth disorders	8
Octreotide	An 8 amino acids synthetic analogue of somatostatin	Acromegaly, psoriasis and gastro-intestinal disorders	9,10
Urokinase	A protein consisting of 411-amino acid residues	A thrombolytic agent	11
Rituxan	A whole antibody with a molecular weight of about 144 kDa	Non-Hodgkin's lymphoma, chronic lymphocytic leukemia	11
sCT	With a molecular weight of 3431 Da and composed of 32 amino acids	Paget's disease	11–14
Polypeptide-k	Contained 9 out of 11 essential amino acids, among a total of 17 types, 168 amino acids	Antidiabetic	15
Dalargin	A model opioid peptide composed of 6 amino acids with a molecular weight of 725 Da	Immunoregulation	16
Elisidepsin	A synthetic marine-derived cyclic peptide	Antitumor	17
Cholera toxin	An oligomeric complex made up of six protein subunits with a molecular weight of 83 kDa	As a neuronal tracer	18
Ovalbumin	Consisted of 385 amino acids and has a relative molecular mass of 42.7 kDa	Used in proteomics and immunology	18–20
BSA	With a molecular weight of 66.5 kDa and composed of 607 amino acids	Often used as a blocker in immunohistochemistry	21–25
Lysozyme	With a molecular weight of 14 kDa and consisting of 130 amino acids	Diarrhea	21,26,27
SOD	A homodimer of molecular weight-33 kDa	Inflammatory bowel diseases	28
Antide	A decapeptide with an antagonist of GnRH	Endometriosis and uterine fibrosis	29
IAPP	A 37-residue peptide hormone	Obesity	30
Irisin	A peptide hormone composed of 111 amino acids	Obesity	30
SIINFEKL (OVA257-264)	A 8-amino-acid peptide	A specific antigenic peptide	31
Exendin-4	A 39-amino-acid peptide	Type 2 diabetes	32–38
GLP-1	A 30 amino acid long peptide hormone	Type 2 diabetes	39,40
Insulin	A dimer of an A-chain and a B-chain composed of 51 amino acids and has a molecular weight of 5808 Da	Diabetes	41–55

hGH, human growth hormone; IAPP, islet amyloid polypeptide; GLP-1, glucagon-like peptide-1; GnRH, gonadotropin hormone-releasing hormone; SOD, superoxide dismutase; BSA, albumin from bovine serum; sCT, salmon calcitonin; EGFR, epidermal growth factor receptor.

intestine leading to a certain number of cargos sticking or aggregating in the partly dissolved shell, which may lower their oral bioavailability. Chuang et al.<sup>61</sup> developed a bubble carrier system which generated nanosized CO<sub>2</sub> bubbles while water passes through the gelatin shell to saturate the compounds and continue to expand till contacting with the mucus and finally burst and liberate the contents. The bubble carrier system produced steady plasma glucose levels (PGL) for over 10 h and a relative bioavailability of 21.7 ± 1.7%. To penetrate through the widely distributed mucus, mucosal adhesive agents as well as mucosal penetrate agents are extensively used. Mucoadhesive materials represented by chitosan (CS), alginate (ALG), methacrylate can be incorporated to prolong the residence time of peptides/proteins in intestine<sup>62</sup>. The highest mucoadhesion was shown by thiolated polymers at pH 3.0. Other tested polymers like cellulose derivatives, polyvinylpyrrolidone and polyethyleneglycole showed low to almost no mucoadhesion<sup>63</sup>. Beyond those strategies applied above, to optimize the efficacy in oral delivery, often the tuning of physicochemical properties like electrical property and particle size is necessary<sup>64</sup>. Surface charge plays a critical role in

the uptake of nanoparticles (NPs) because of the anionic intestinal barrier. Czuba et al.<sup>65</sup> proved that formulation of negatively charged NPs represents a promising approach to improve NPs' uptake and oral bioavailability of Ins. Furthermore, particle size is thought to be a critical factor affecting the bioavailability of NPs following oral exposure since larger size may be intercepted by the steric barriers of mucosal network. Barbari et al.<sup>66</sup> prepared ultrasmall (<15 nm), monodispersed and water-dispersible NPs applying a simple and reproducible water-in-oil (w/o) nanoemulsion technique. Results exhibited 15%–19% enhanced transshipment of Ins across the cell monolayer. He et al.<sup>67</sup> reported a new method, termed flash nanocomplexation (FNC), to fabricate smaller size (45 nm) and higher encapsulation efficiency (EE, >90%) of Ins loaded NPs by infusing aqueous solutions of CS, tripolyphosphate (TPP), and Ins under rapid mixing condition ( $r > 1600$ ) in a 4-inlet vortex mixer. Results showed that smaller NPs could regulate the PGL more effectively than the larger. When evaluating particle characteristics that influence their uptake, agglomerate state in the GIT must be assessed. Hinkley et al.<sup>68</sup> demonstrated that different from uncoated

gold NPs that are tend to be agglomerated, polyethylene glycol (PEG)-coated gold NPs can be observed as primary, un-agglomerated particles throughout the GIT using transmission electron microscopy (TEM). Strategies of co-administration with protease inhibitors (PIs) such as aprotinin and calcium chelators could help NPs safely undergo the enzymes in GIT. However, relatively high doses of the PIs may cause safety dangers following repeated administrations<sup>69</sup>. To pass the epithelial barriers two strategies applied have achieved considerable successes: paracellular pathway by opening TJs and transcellular transcytosis ways by clathrin-mediated endocytosis, caveolae-mediated endocytosis, macropinocytosis or phagocytosis<sup>70</sup>. The primary approaches that the peptides/proteins loaded NPs traverse the intestinal epithelium are manifested in Fig. 2. Strategies of co-administration with penetrate enhancers (PEs) such as bile salts, fatty acids, surfactants, CS and derivatives, chelating agents and other enhancers could help traverse poorly penetrating intestinal barriers in GIT<sup>69</sup>. For instance, Gaowa et al.<sup>5</sup> prepared epidermal growth factor receptor (EGFR)-targeted hybrid peptide/bile acid complexes *via* electrostatic interactions. The *in vitro* permeability of the complexes across Caco-2 cell monolayers was 5.0-fold higher than free peptide.

Furthermore, after treated with the complexes *in vivo*, the mean tumor volume reduced 1.6-fold than that of the free peptide. Cell-penetrating peptides (CPPs) composed of 5–30 amino acid residues have been investigated for several years as PEs through electrostatic or covalent conjugation with hydrophilic macromolecules for oral delivery<sup>71</sup>. The most extensively applied synthetic CPPs include MAP, octa-arginine (8R), CADY, and polylysine. CPP-mediated delivery has been reported to take place *via* multiple endocytosis ways including macropinocytosis, caveolae mediated and clathrin-mediated pathways<sup>72</sup>. In addition, more efficient and specific delivery can be realized by incorporating actively targeted ligands into CPP based systems. There are a variety of special receptors such as vitamins, transferrins, amino acids and sugar receptors expressing on the epithelium of intestine<sup>73</sup>. Being more effective with low poisonous, strategies containing targeted ligands *via* receptor-mediated transport have become the major impetus towards the oral delivery that can overcome the intestinal barriers<sup>74,75</sup>. Representative ligand-mediated transports in oral delivery are shown in Table 3. In addition, drug co-loading technique can be applied to enhance the therapeutic effect and bioavailability of peptides. Araújo et al.<sup>39,40</sup> orally co-delivered

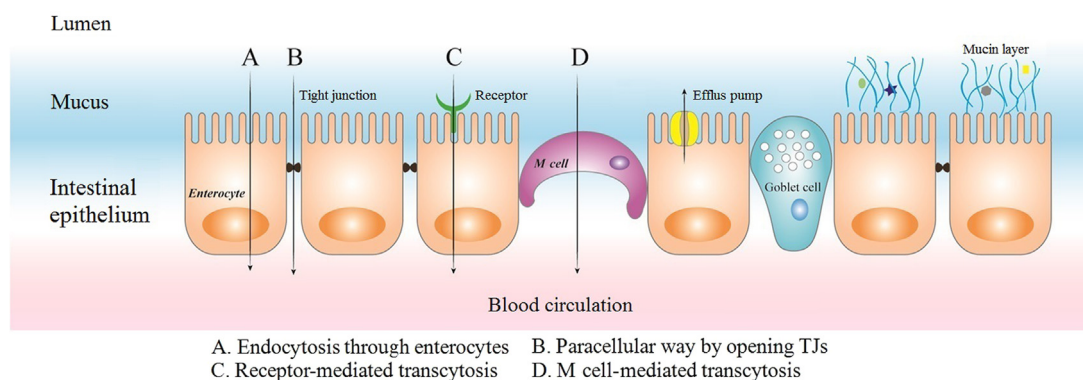


**Figure 2** Primary approaches for the peptides/proteins loaded nanoparticles traversing the epithelium.

**Table 3** Representative ligand-mediated transport in oral delivery of therapeutic peptides/proteins.

Name	Distribution/Function	Characteristics	Ref.
Bile acid transporters	In the epithelium of ileum	The ASBT in the small intestine transports bile acids into epithelial cells for bile acid recycling	5,48,52,76–81
UEA-1	In M-cell	M-cell selective molecular signature	20
Lectin-like protein receptors	In the intestine	Proteins or glycoproteins specifically recognize the carbohydrate moieties on the intestine	42
Biotin (vitamin B7) receptor	In the intestine	The biotin receptor distributes throughout the small intestine	55
Proton-coupled oligopeptide transporters PepT1 and PepT2	In the brush border membrane of the small intestine	Driven by the presence of an inward H <sup>+</sup> gradient and a negative membrane potential. Transports various natural di/tri-peptides and comprehensive peptide-mimetics. High capacity, low affinity	82,83
CSK peptide transporters	In goblet cells	CSK peptide specifically recognize goblet cells	84
AT-1002 peptide	Open TJs	A hexamer peptide derived from ZOT open the TJs transiently and reversibly	85
Monocarboxylate transporter	In the intestine	Cellular uptake of SCFAs efficiently, among which butyrate is in majority, a key mediator of physiological function in the intestine	86
CD44 receptor	In the intestine	A highly heterogeneous single-stranded transmembrane glycoprotein widely expressed on the membrane	87

ASBT, apical sodium-dependent bile acid transporter; CSK, CSKSSDYQC; ZOT, zonula occludens toxin; TJs, tight junctions; UEA-1, ulex europaeus agglutinin-1; SCFAs, short chain fatty acids.

glucagon-like peptide-1 (GLP-1) and dipeptidyl peptidase 4 inhibitor (DPP4I) by a multifunctional tailorable composite system. In the presence of DPP4I, the permeability of GLP-1 across the cell monolayers was even higher, with 1.5-fold increase for the porous silicon (PSi) systems and 5-fold increase for the poly(lactide-co-glycolide) (PLGA) systems.

Above all, we can see that versatile formulation strategies have been evolved to enhance the oral bioavailability of peptides/proteins. The objective of our review is to put forward a systematic overview on recently published promising delivery systems represented by lipid-based particles, polysaccharide-based particles, inorganic particles, and synthetic functional particles for oral delivery of therapeutic peptides/proteins. Typical structures of peptides/proteins carriers are demonstrated in Fig. 3. These works are in particular concerned with formulation strategies for controlled drug release, meliorative pharmacokinetics/pharmacodynamics and other modulated physicochemical characteristics. Several novel techniques developed to optimize the preparation of oral delivery carriers are shown in Table 4. We also discuss the strategies to enhance the oral bioavailability of peptides/proteins and make suggestions for further design in oral delivery systems (Figs. 4–6).

## 2. Lipid-based particles

Lipid-based carriers have attracted much attention for their excellent biocompatibility to cross the intestinal barrier<sup>89,90</sup>. Summary of lipid-based particles applied in oral delivery of therapeutic peptides/proteins was shown in Table 5.

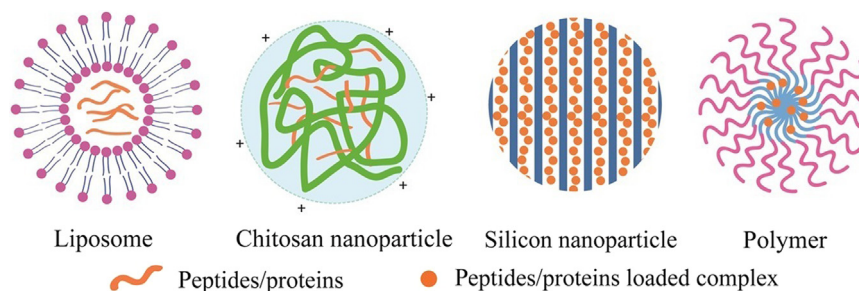


**Figure 3** Typical structures of peptides/proteins loaded nanocarriers.

**Table 4** Novel techniques for oral delivery of therapeutic peptides/proteins.

Experimental Techniques	Advantages/Improvements	Ref.
CARS microscopy	To image protein and lipid distributions without prior labeling or destructive sample preparation	26
Microfluidics technique	Emulsions are formed with an exquisite control and a quite high encapsulation efficiency compared to the conventional production methods	39,40
Oral dual-delivery of GLP-1 and DPP4 inhibitor	The permeability of GLP-1 across the cell monolayers was higher while coloaded DPP4 inhibitor	39,40
A novel w/o nanoemulsion technique	A simple and reproducible technique making ultrasmall (< 15 nm), monodispersed and water-dispersible NPs	66
FNC	The optimized FNC process produces NPs with a smaller size (45 nm) and higher encapsulation efficiency (90%) compared with the bulk-mixing method	67
Three-layer release technology	The platform consisting of neutral polymethacrylate Eudragit <sup>®</sup> NE as a flexible film, superdisintegrant sodium starch glycolate Explotab <sup>®</sup> as a pore former and applied to a HPMC coating of reduced thickness delays the drug release.	88

GLP-1, peptide glucagon-like peptide-1; DPP4, dipeptidyl peptidase 4; NPs, nanoparticles; CS, chitosan; CARS, coherent anti-stokes Raman scatterer; HPMC, hydroxypropyl methylcellulose.

### 2.1. Liposomes

Liposomes with micro-vesicular structures are composed of aqueous cores and amphiphilic bilayers. Considering that conventional phospholipid/cholesterol liposomes are compromised to the hostile environment in GIT by phospholipid hydrolysis or oxidation and moreover restricted by aggregation, sedimentation, and fusion<sup>91</sup>, well-designed liposomes are extremely essential for effective delivery.

Niu et al.<sup>52,80,81</sup> compared the effect of three kinds of liposomes loaded with SGC, sodium taurocholate (STC) or sodium deoxycholate (SDC). The hypoglycemic effect was size-dependent with the highest at 150 or 400 nm and oral bioavailability were in the order of SGC ( $8.5 \pm 2.1\%$ ) > STC > conventional liposomes > SDC. Liposomes containing bile salts showed prolonged residence time and enhanced permeation across the membranes. They further investigated the transiting fate of bile acid-liposomes and verified the absorption of intact liposomes rather than free Ins. Additionally, ergosterol was found to be a substitute for cholesterol and bile salt derivatives in liposomes. Cui et al.<sup>92</sup> screened liposomes contained ergosterol (Er-Lip) of botanical origin rather than cholesterol as the stabilizer. Results indicated that Er-Lip was more stable and enhanced oral bioavailability of Ins more significantly. Thiomers-coated liposomes present favorable characteristics of mucoadhesion, TJs-opening effect, efflux pumps inhibition, and enzyme inhibition<sup>93–95</sup>. Gradauer et al.<sup>14</sup> coupled CS and thioglycolic acid (TGA) to coat sodium calcitonin (sCT)-loaded liposomes, these thiomers-coated liposomes causing no immunogenic reactions in mice showed enhanced permeation of

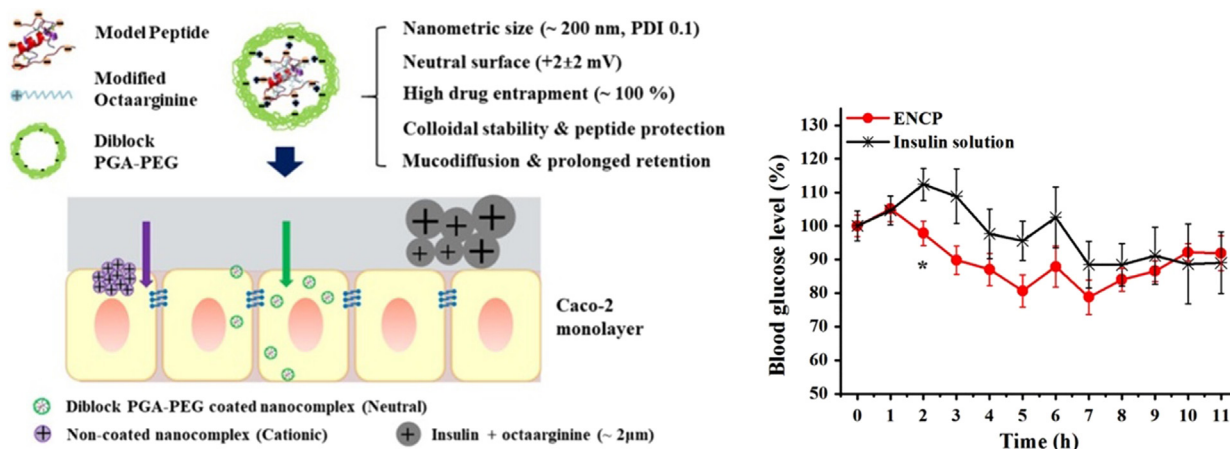


**Figure 4** Schematic illustration of rational design of octaarginine-based nanoparticles and their hypoglycemic effect in rats<sup>78</sup>. Adapted from Niu et al.<sup>168</sup> with permission © 2018 Elsevier Ltd.

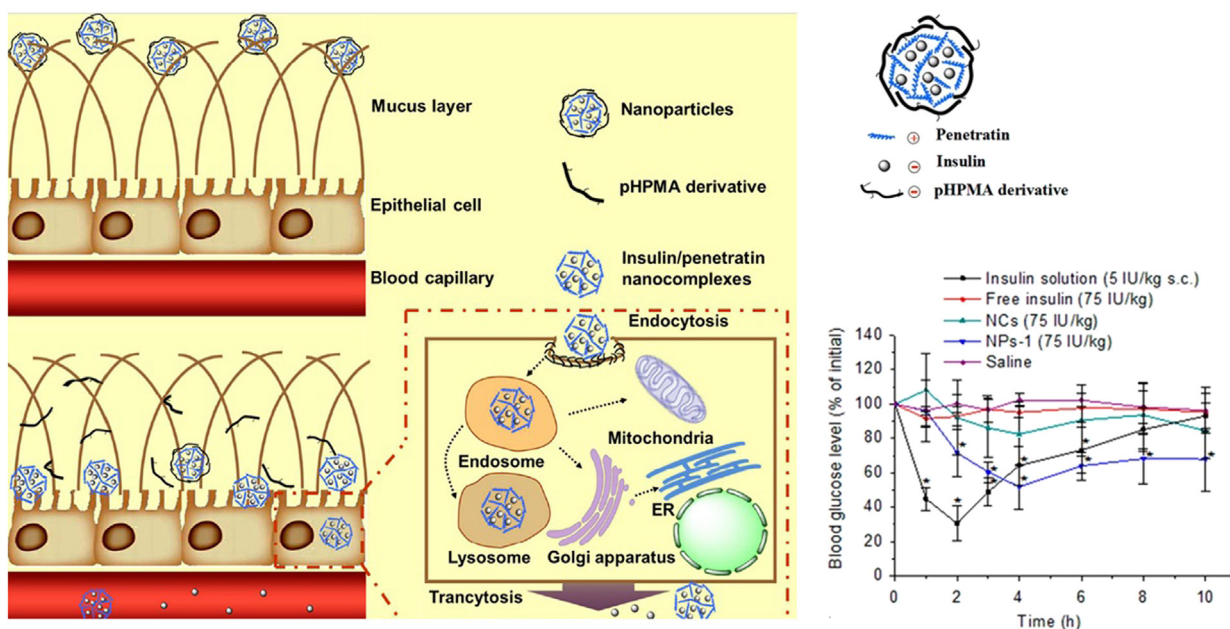


**Figure 5** Schematic illustration of the self-assembled NPs overcoming the mucus barrier and epithelium barrier<sup>163</sup>. Adapted from Shan et al.<sup>163</sup> with permission © 2015 American Chemical Society.

membranes and inhibitory properties of efflux pump. These coated liposomes reduced the blood calcium level to a minimum of 65% of the initial value after 6 h. Comparing the areas under curves (AUC) of the blood calcium levels, these coated liposomes led to an 8.2-fold increase compared to the free sCT solution. Biotin (vitamin B7) is a promising ligand for oral delivery because its receptor distributes throughout the small intestine. Through the incorporation of biotin-conjugated 1,2-distearoyl-*sn*-glycero-3-phosphatidyl ethanolamine (DSPE) into the liposome membranes, Zhang et al.<sup>55</sup> produced biotinylated liposomes (BLPs) for oral delivery of Ins and this BLPs achieved a relative bioavailability of 12.09%, approximately twice than that of conventional liposomes.

To enhance the oral bioavailability of encapsulated peptides/proteins, liposomes should maintain their vesicular form and avoid early leakage of loaded cargos by withstanding the destruction of

bile salts, pancreatic enzymes and the acidic conditions in GIT<sup>96</sup>. Separated from prokaryotic microorganisms, archaea with unique membrane lipids can survive extreme environments in GIT. These tetraether lipids containing membrane spanning hydrocarbon chains linked through ether bonds are much more stable than conventional phospholipids in harsh circumstances. Two major groups of archaeal membrane lipids are known as diphytanyl-glycerol diether lipids (DELs) and its derivatives, dibiphytanyl-glycerol tetraether lipids (TELs) and its derivatives. Parmentier et al.<sup>97</sup> tested *in vitro* that particular TEL-glycerylcaldityl tetraether (GCTE)-stabilised liposomes could maintain the integrity of membrane and protect encapsulated proteins from degradation. They further confirmed that the relative oral bioavailability of human growth hormone (hGH) loaded tetraether lipids containing cetylpyridinium chloride (CpCl) as a bio-enhancer was around

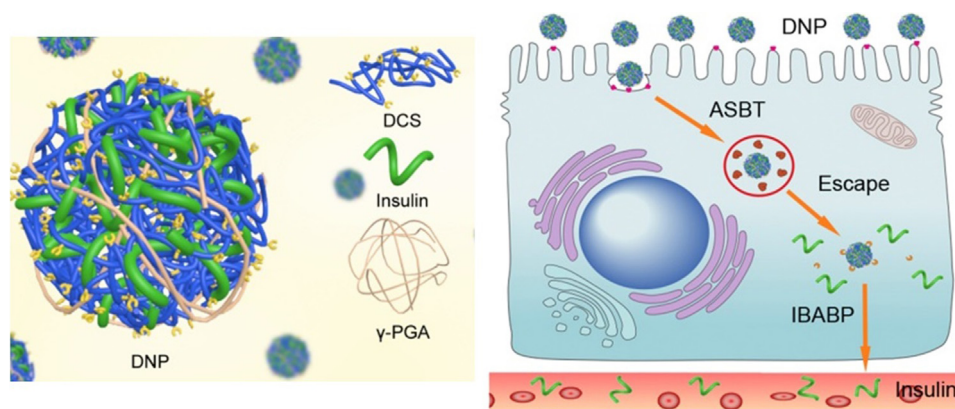


**Figure 6** Schematic illustration of transepithelial transport of Ins from DNP to overcome multiple barriers of the intestinal epithelium by exploiting the bile acid pathway<sup>168</sup>. Adapted from Fan et al.<sup>78</sup> with permission © 2017 Elsevier Ltd.

3.4% whereas free hGH administered orally was only 0.01%<sup>8</sup>. What's more, liposomes with 25% TEL could improve the oral bioavailability of octreotide more than 4-fold compared with free octreotide<sup>9</sup>. Uhl et al.<sup>6</sup> found that an almost two-fold elevation in vancomycin uptake of TEL-liposomes over conventional liposomes was detected in Wistar rats. He and his group<sup>28</sup> further showed that myrcludex B-loaded GCTE-liposomes contributed 1.6-fold higher of relative oral bioavailability than the standard liposomes. Proliposomes, prepared by adsorption of drug and phospholipids on to the carriers having microporous matrix like mannitol and sorbitol, are free-flowing powdered particles superior to conventional liposomes. Sharma et al.<sup>98</sup> employed protamine sulphate (Pt) as a PE and prepared Pt-rhIns proliposomes encased in Eudragit S100, which ameliorated the cellular uptake of rhIns almost 4.0-fold compared to free rhIns.

The fate of these nanocarriers (NCs) after oral delivery is still unknown, which can be explained by the difficulty to find relevant approaches to confirm the real integrity of the carriers, that is whether the cargos are still inside the carriers or not. Indeed, several techniques such as dynamic light scattering (DCS), confocal laser scanning microscopy (CLSM) and Fourier transform infrared spectroscopy (FTIR) could characterize the whole structure of carrier or its individual parts but not the integrity. A novel technique, Förster resonance energy transfer (FRET), which is highly sensitive to donor–acceptor distances and indicates preserved nanoscale environment can quantify the integrity of nanocarriers<sup>99</sup>. Roger et al.<sup>100</sup> studied the fate of lipid nanocapsules after their transportation across Caco-2 cell model employing FRET and Nanoparticle Tracking Analysis. Results showed that the presence of NPs in the basolateral side have a measurable FRET signal after 2 h, which verifies the intact crossing of the NCs.

## 2.2. Solid lipid particles

Solid lipid particles (SLPs) are made of natural, semi-synthetic or synthetic lipids containing triglycerides, fatty acids, partial glycerides, phospholipids and steroids, which are widely considered as safe and biodegradable<sup>101</sup>.

Christophersen et al.<sup>26,27</sup> investigated that the SLPs with different types of lipid excipients exhibited a lipase-mediated degradation mechanism on release of proteins. He and his colleagues further proved that lysozyme incorporated SLPs in an aqueous solution released lysozyme much faster than in a solid.

However, the hydrophobic nature of SLPs limits its encapsulation of hydrophilic peptides accounting for low EE. Hecq et al.<sup>102</sup> dissolved Ins into the inner aqueous phase and then emulsified in an organic phase to prepare a bioadhesive cationic SLPs, which increased 2.5-fold the transshipment of capped Ins through co-cultured Caco-2/HT29 cells compared to free Ins. Boushra et al.<sup>103</sup> adopted three different hydrophilic viscosity-enhancing agents (VAs): propylene glycol (PG), PEG 400 and PEG 600 within SLP cores to develop Ins-loaded NCs with enhanced viscosity. The highest EE was achieved by 70% (*w/w*) PG contained NCs (54.5%) compared to only 20.4% in unmodified SLN and achieved good hypoglycemic effect with a relative bioavailability of 5.1% following oral administration. It should be noted that the mucosal layer has a significant impact on determining the efficiency of oral nanoformulations. It is also shown that low MW and high surface coverage of PEG could minimize mucoadhesion and enhance the hydrophilic of SLPs. Yuan et al.<sup>104</sup> evaluated that the permeation ability of PEGylated (MW = 2 kDa) SLPs were decreased through Caco-2 cell monolayer while increased through a mucus-secreting co-cultured Caco-2/HT29 cells. The relative oral bioavailability of PEGylated SLPs elevated 1.99-fold compared to unmodified ones.

## 2.3. Self-nanoemulsifying drug delivery system (SNEDDS)

SNEDDS is an (o/w) nanoemulsion spontaneously formed by isotropic mixtures of oil, surfactant and cosurfactant through mixing with water<sup>105</sup>.

Karamanidou et al.<sup>49</sup> developed a new mucus permeating SNEDDS formulation, incorporating a hydrophobic ion pair of Ins/dimyristoyl phosphatidylglycerol (DMPG), which exhibited enhanced mucus penetration and an EE of 70.89%. Li et al.<sup>106</sup> prepared Ins–phospholipid complex-loaded SNEDDS and then coated with Eudragit<sup>®</sup> L100, the EE of which was increased from 18.6% of single Ins to 73.1%. Oral administration of complex-loaded SNEDDS enhanced 2.7-fold the relative bioavailability and 3.4-fold the reduction of PGL separately compared to Ins-loaded carriers. Garg et al.<sup>15</sup> designed a successful SNEDDS for oral delivery of polypeptide-k (PPK) which exhibited stable characters and promising antidiabetic potentials compared to its native form. It is reported that smaller SNEDDS have higher mucus permeating abilities and anionic SNEDDS demonstrated a better permeation rate than positively charged ones<sup>107</sup>. Recently, several studies are focusing on the protective effects against protease degradation.

**Table 5** Summary of lipid-based particles in oral delivery of therapeutic peptides/proteins.

Formulation composition	Model drug	Main transport mechanisms	Characterization (size, ZP, EE)	PK		PD	Ref.
				Dose	<i>F</i> (%)		
GCTE-liposomes	Vancomycin	N/A	Size: 134.0±9.7 nm; ZP: -4.43±0.81 mV; EE: 58.53±1.76%	N/A	N/A	N/A	6
GCTE-liposomes	Myrcludex B	N/A	Size: 140.7±4.3 nm; ZP: -4.20±0.48 mV; EE: 65.67±2.91%	N/A	N/A	3.5-Fold increase compared to the free peptide	7
Liposomes containing bio-enhancers and tetraether lipids	hGH	N/A	Size: 229.7±12.8 nm; ZP: 41.0±1.2 mV; EE: 31.2±0.5%	8 mg	3.4	N/A	8
Liposomes with 25% TELs	Octreotide	N/A	Size: 130–207 nm; EE: 13.0%	N/A	N/A	4-Fold the hypoglycemic effect compared with free octreotide	9
Octreotide-DOCA SEDDS	Octreotide	N/A	Size: 152 nm; ZP: -3.7 mV	50 mg (pig)	5.21	N/A	10
CS-TGA-MNA-coated liposomes	sCT	TJs opening	Size: 604.8±29.6 nm; ZP: 27.9±1.1 mV	40 µg	4.04	A minimum of 65% of PGL value after 6 h	14
Exenatide/DOC SNEDDS	Exendin-4	N/A	Size: 45.87±2.9 nm; ZP: 0.7±0.1 mV	150 µg	14.62±3.07	20.6% decrease of PGL in 5 h	38
Liposomes containing SGC, STC, STC respectively	Ins	Transcellular way	Size: 157±19 nm; EE: 29.8±1.7% (the optimal formulation)	20 IU/kg	8.5±2.1 (the optimal formulation)	60% decrease of PGL in 20 h with peak time around 8–12 h	52,81
Biotinylated liposomes (BLPs)	Ins	Biotin receptor mediated transport	Size: ~150 nm; EE: 35%–42%	20 IU/kg	12.09	64% reduction of the PGL in 24 h with peak time around 5–12 h	55
Proliposomes encased in Eudragit S100	Ins	Paracellular way	Size: 583.2±10.2 nm; ZP: 28.3±3.7 mV; EE: 17.6±2.4%	N/A	N/A	N/A	98
VA incorporated SLN nanoparticles	Ins	N/A	Size: 172~281 nm; ZP: -40 mV; EE: 54.5%	50 IU/kg	5.1	~50% decrease of PGL in 4 h	103
Ins-phospholipid complex loaded SNEDDS	Ins	TJs opening	Size: multi-dispersed peaks; ZP: -4.1±0.3 mV ; EE: 73.1%	50 IU/kg	0.43±0.13	38% decrease of PGL in 10 h	106

ZP, zeta potential; EE, encapsulation efficiency; *F*, relative bioavailability; PGL, plasma glucose levels; TGA, thioglycolic acid; MNA, 6-mercaptopnicotinamide-conjugate; Pt, protamine; TELs, tetraether lipids; GCTE, glycerylcaldityltetraether lipids; VA, viscosity-enhancing agent; SNEDDS, self-nanoemulsifying drug delivery systems; DOC, sodium docusate; DOCA, deoxycholate



Hetényi et al.<sup>108</sup> verified that SNEDDS provided a perfect protection towards protease degradation and deactivation by GSH. Zupancic et al.<sup>16</sup> evaluated SNEDDS for oral delivery of a opioid peptide, dalargin. Results showed that the established SNEDDS exhibited mucus penetrating properties and protective effects against enzymatic degradation by trypsin,  $\alpha$ -chymotrypsin, and elastase, etc. Menzel et al.<sup>38</sup> developed an oral SNEDDS loading exenatide *via* hydrophobic ion pairing with sodium docusate (DOC). After oral administration, exenatide/DOC SNEDDS showed a relative bioavailability of  $14.62 \pm 3.07\%$  and caused a significant ( $P < 0.05$ ) decrease in PGL. Bonengel et al.<sup>10</sup> investigated the impact of different hydrophobic ion pairs (SDC, decanoate and docusate) for SNEDDS on the oral bioavailability of octreotide in pigs. *In vivo* studies showed that octreotide–SDC and octreotide–docusate SNEDDS resulted in 17.9-fold and 4.2-fold higher bioavailability separately than free octreotide. According to these results, hydrophobic ion pairing might be an important factor for SNEDDS to elevate the oral bioavailability.

Despite all this, SNEDDS used to deliver hydrophilic drugs including therapeutic peptides/proteins is considered extremely challenging due to their hydrophobic nature.

#### 2.4. Multiemulsion

Multiemulsions, liquid or semisolid disperse systems of a simple emulsion in an external phase, can protect drug from enzymatic hydrolysis and increase absorption through the intestinal barriers as drug carriers<sup>109</sup>.

Dogru et al.<sup>110</sup> designed a w/o/w multiple emulsion formulation for oral delivery of sCT, which produced analogous effects of serum calcium compared to the commercial preparations in rats. Venkata et al.<sup>111</sup> prepared Ins-loaded NPs in multiemulsion with particle size of 300–400 nm, which, in different pH conditions, protected cargos from destruction. Griffin et al.<sup>112</sup> prepared Ins-loaded tripalmitin nanoparticles by water/oil/water (w/o/w) multiple emulsion technique. The nanoparticles coated by PEG–stearate were proved to be more stable from pancreatin. Li et al.<sup>113</sup> prepared w/o/w nanoemulsions coated with alginate/chitosan, which demonstrated great protection for Ins in SIF and the bioavailability of Ins was 8.19%. Agrawal et al.<sup>114</sup> formulated Ins entrapped Eudragit S100 microspheres by w/o/w multiemulsion solvent evaporation technique, which showed a relatively high EE (76.84%) and pH-dependant controlled release. Although multiemulsion is a common approach for oral delivery of peptides/proteins, the main drawbacks of instability and increased particle sizes restricts its development.

### 3. Polysaccharide-based delivery systems

Polysaccharides are considered as highly safe, biocompatible, and biodegradable natural biomaterials with high MW. Most polysaccharides have hydrophilic groups such as hydroxyl, carboxyl, and amino groups, which could form non-covalent bonds with intestinal mucus to facilitate the absorption of therapeutic peptides/proteins<sup>115</sup>. Summary of polysaccharide-based delivery systems applied in oral delivery of therapeutic peptides/proteins are shown in Table 6.

#### 3.1. Chitosan and its derivatives

Obtained from alkaline deacetylation of chitin, CS is a polycation copolymer ( $pK_a = 6.5$ ) composed of *N*-acetyl glucosamine (Glc-

NAc) and glucosamine (GlcN) presenting pH responsive property with low poisonousness, which embraces mucoadhesion by interacting with anionic sialic acid residues on mucosal surfaces and permeation enhancing effect by reversibly opening TJs. CS-based NPs are attracting increased attentions for their abilities to orally deliver therapeutic peptides/proteins. Poly- $\gamma$ -glutamic acid ( $\gamma$ PGA), a natural peptide carrying negative charge, has been used to deliver protein vaccines. Sonaje et al.<sup>54</sup> prepared Ins-loaded CS NPs mixing with anionic  $\gamma$ PGA with a mean particle size of  $218.0 \pm 3.4$  nm and EE of  $71.8 \pm 1.1\%$ . During the preparation of NPs,  $MgSO_4$  and TPP were introduced to raise their stabilities in an extensive range of pH. The NPs demonstrated a relative bioavailability of  $15.1 \pm 0.9\%$  and a reductive trend in PGL in 10 h in diabetic rats. It is well known that divalent metal ions play a key role in developing the apical junctions and preserving protease activity. Diethylene triamine pentaacetic acid (DTPA), a complexant, is able to disrupt TJs and restrain protease activity by chelating divalent metal ions. Su et al.<sup>116</sup> covalently conjugated DTPA on  $\gamma$ PGA mixing with CS for oral delivery of Ins. The CS/ $\gamma$ PGA NPs protected the loaded cargos from enzymatic attacks and kept intact when  $pH < 7.0$  in the intestine, which *in vivo* achieved a relative bioavailability of  $19.7 \pm 1.3\%$ . Besides, ethylene glycol tetraacetic acid (EGTA) is a  $Ca^{2+}$ -specific chelating agent. Chuang et al.<sup>117</sup> synthesized CS/ $\gamma$ PGA–EGTA NPs for oral delivery of Ins, which ultimately produced a prolonged hypoglycemic effect *in vivo* with a relative bioavailability of  $21.3 \pm 1.5\%$ . They further demonstrated that combination therapy by co-loading Ins with exendin-4 delivered by CS/ $\gamma$ PGA NPs can be more effective than its monotherapy counterparts in achieving preferable glycemic control and undergoing oral glucose tolerance test (OGTT)<sup>118</sup>. It is well known that CS NPs with smaller size demonstrated better absorption and transportation in GIT. Apart from size, the MW and deacetylation degree of CS in NPs also associated with its performance and stability<sup>119</sup>. Sukyung et al.<sup>33</sup> conjugated cysteinylated exendin-4 to low molecular weight chitosan (LMWC) *via* a disulfide bond which is cleavable under *in vivo* circumstances. The LMWC–exendin-4 conjugate have a mean particle size of  $101 \pm 41$  nm and a relative bioavailability of 6.4%. Besides, surface charge properties may determine the absorption sites of NPs in small intestine. Two Ins-loaded CMCS/CS nanogels (NGs) with similar shape, size, but opposite surface charge were prepared by Wang et al.<sup>120</sup>. The negatively charged NGs exhibited a higher mucoadhesion and better intestinal permeability than positively charged ones in *ex vivo* intestinal studies, which can be accounted for the attenuated surface charge of CMCS/CS-NGs (+) and weaker contact with mucosal epithelium in alkalescence environment ( $pH > 6.5$ ) of jejunum. It is known that transition metal ions such as  $Fe^{3+}$  may form coordinate-covalent bonds with glycosidic, carboxylic, and hydroxyl oxygen atoms, which could be used to increase the EE of NPs. Nguyen et al.<sup>34</sup> prepared CS/ $\gamma$ PGA NPs, in the presence of  $Fe^{3+}$ , the EE of NPs significantly enhanced 2.5-fold compared to NPs without  $Fe^{3+}$ . Oral administration of the NPs increased the blood level of Ins in a slower but prolonged manner in 12 h and the bioavailability, *versus* the s.c. counterpart, was found to be  $14.0 \pm 1.8\%$ . However, the oral bioavailability of peptide-loaded NPs is still far from satisfactory. One main reason is the fast leakage of cargos from the NPs in GIT. Therefore, to improve the oral bioavailability, peptides should not only be protected from enzymatic digestion, but also possess the ability to traverse the epithelial barriers. Ins–LMWP conjugates were prepared by Sheng et al.<sup>121</sup> and then loaded into trimethyl chitosan (TMC)-coated

**Table 6** Summary of polysaccharide-based particles in oral delivery of therapeutic peptides/proteins.

Formulation composition	Model drug	Main transport mechanisms	Characterization (size, ZP, EE)	PK		PD	Ref.
				Dose	F (%)		
Matrix tablets prepared by 6-MNA protected TGA-CS	Antide	Paracellular way	N/A	2 mg	10.88 ± 4.22	N/A	29
BSA/dextran NPs cross-linked with STMP	Exendin-4	Lymphatic uptake (not confirmed)	Size: 192.7 ± 3.5 nm; ZP: 39.5 mV	165 µg/kg	77	N/A	32
Conjugated with LMWC through disulfide bonds	Exendin-4	N/A	Size: 101 ± 41 nm; ZP: 44.36 mV	400 µg/kg	6.39	22.90 ± 2.0% decrease of PGL in 3 h for 4 µg/kg, while 41.07 ± 4.7% for 40 µg/kg	33
CS/Fe <sup>3+</sup> -γ-PGA NPs	Exendin-4	Paracellular way	Size: 260.6 ± 26.4 nm; EE: 60.92%	300 µg/kg	14.0 ± 1.8	25% decrease of PGL in a slower but prolonged manner in 12 h	34
CS/TPP	Exendin-4	Paracellular way	Size: 303.1 ± 10.36 nm; ZP: 18.37 ± 1.15 mV; EE: 38.02.6%	N/A	N/A	N/A	37
PLGA/CS-CPP (PSi/CS-CPP)	GLP-1coloaded with DPP4 inhibitor	N/A	Size: 277.2 ± 3.8 nm (320.0 ± 9.8 nm); ZP: 21.6 ± 3.8 mV (19.1 ± 1.0 mV); EE: 59.7 ± 0.7% (75.0 ± 0.5%)	N/A	N/A	44% decrease of PGL in 8 h	39,40
CS/γ-PGA	Ins	Paracellular way	Size: 218.0 ± 3.4 nm; ZP: 25.3 ± 0.9 mV; EE: 71.8 ± 1.1%	30 IU/kg	15.1 ± 0.9	Low impact on PGL	54
DOCA-modified CS nanoparticles	Ins	Bile acid receptor-mediated transport	Size: ~226.1 nm; ZP: 9.4 mV	30 IU/kg	15.9	A slower but prolonged 50% reduction of PGL in 12 h	78
TMC-CM-GG and TMC-CM-AA NPs	Ins	Opening TJs and actively transported by oligopeptide transporters	Size: 157.3–197.7 nm; ZP: 24.35–34.37 mV; EE: 70.60–86.52%	20 IU/kg	17.19	45.1% decrease of PGL in 8 h of TMC-CM-AA NPs	82
CMCS-PBA-LV	Ins	Paracellular way and transcellular way	EE: 67%	75 IU/kg	7.55 ± 1.32	60% decrease of PGL in 12 h	83
PGA-g-DA micelles with CSK peptide conjugated TMC	Ins	Clathrin-dependent and caveolae-dependent endocytosis	Size: 184.5 ± 13.5 nm; ZP: 24.70 ± 2.45 mV; EE: 83.51 ± 4.24%	50 IU/kg	7.05	50% decrease of PGL in 12 h, totally 1.19-fold higher than T-NPs	84
AT-1002 peptide-CS dual pluronic-based nanocarrier	Ins	TJs opening	Size: ~150 nm; ZP: 20.0 ± 3.4 mV; EE: >95%	75 IU/kg	~10	~50% decrease of PGL in 20 h	85
CS/γ-PGA-DTPA NPs	Ins	Paracellular way	Size: 246.6 ± 4.8 nm; ZP: 37 ± 0.3 mV; EE: 75.7 ± 0.7 %	30 IU/kg	19.7 ± 1.3	50% decrease of PGL in 10 h	116

Table 6 (continued)

Formulation composition	Model drug	Main transport mechanisms	Characterization (size, ZP, EE)	PK		PD	Ref.
				Dose	F (%)		
CS/ $\gamma$ -PGA-EGTA NPs	Ins	Paracellular way	Size: $328.6 \pm 2.3$ nm; ZP: $38.7 \pm 0.2$ mV; EE: $78.7 \pm 0.4\%$	30 IU/kg	$21.3 \pm 1.5$	60% decrease of PGL in 12 h	117
PLGA/FA-CS	Ins	N/A	Size: $252.4 \pm 4.6$ nm; ZP: $5.99 \pm 2.85$ mv; EE: 41%	70 IU/kg	$7.77 \pm 1.3$	50% decrease of PGL in 12 h	128
TMC/ pHPMA	Ins	TJs opening	Size: $163.1 \pm 3.99$ nm; ZP: $-3.35 \pm 1.0$ mv; EE: $54.1 \pm 1.9\%$	50 IU/kg	8.56	36% decrease of PGL in 4 h	131
PSA coated protamine NCs	Ins	Paracellular way and caveolae (predominantly) and Clathrin mediated endocytosis	Size: $301 \pm 84$ nm; ZP: $-4 \pm 1$ mV; EE: $51 \pm 9\%$	N/A	N/A	20% decrease of PGL in 9 h	135
CS/ALG	Ins	TJs opening	Size: 104 nm; ZP: $+3.89$ mV; EE: 78.3%	50 IU/kg	$\sim 8.11$	70% decrease of PGL in 9 h	136
Dual chitosan/albumin-coated alginate/dextran sulfate nanoparticles	Ins	Clathrin-mediated endocytosis.	Size: $300.8 \pm 3.8$ nm; ZP: $28.9 \pm 0.9$ mV; EE: $30.7 \pm 3.4\%$	N/A	N/A	N/A	138
CS/HPMCP	Ins	Paracellular pathway and adsorptive endocytosis and in part by clathrin-mediated vesicles	Size: 255 nm; ZP: $30.1 \pm 0.8$ mV; EE: $60.88 \pm 1.09\%$	12.5 U	$8.47 \pm 1.59$	60% decrease of PGL in 12 h	140
HP55-coated capsule containing PLGA/RS NPs	Ins	N/A	Size: $285.6 \pm 4.5$ nm; ZP: $+42.9 \pm 1.4$ mV; EE: 73.9%	50 IU/kg	$9.2 \pm 2.4$	40% decrease of PGL in 15 h	142
PAA/S-CS hydrogel	Ins	N/A	EE: $\sim 76\%$	50 IU/kg	$\sim 4.43$	$\sim 55\%$ decrease of PGL in 6 h	144

ZP, zeta potential; EE, encapsulation efficiency; F, relative bioavailability; PGL, plasma glucose levels; NPs, nanoparticles; TMC, trimethyl chitosan; TMC-CM-GG, glycyl-glycine conjugated nanoparticles; TMC-CM-AA, alanyl-alanine conjugated nanoparticles; TJs, tight junctions; INS, insulin; TPP, sodium tripolyphosphate; CS, chitosan; NCs, nanocomplexes;  $\gamma$ -PGA, poly- $\gamma$ -glutamic acid; DTPA, diethylene triamine pentaacetic acid; GLP-1, glucagon-like peptide-1; DPP4, dipeptidyl peptidase 4; PEs, permeability enhancers; BSA, bovine serum albumin; STMP, sodium trimetaphosphate; LMWC, low molecular weight chitosan; PSi, mesoporous silicon; CPP, cell penetrating peptides; CMCS, carboxymethyl chitosan; PBA, phenylboronic acid; LV, L-valine; LMWH, low molecular weight heparin; DOCA, sodium deoxycholate; ASBT, sodium-dependent bile acid transporter; PSA, polysialic acid; BGL, blood glucose level; C12, lauric acid; Chol, cholesterol; r8, octaarginine; SGC, sodium glycocholate; TMC, N-trimethylated chitosan; CS-6-MNA, chitosan-6-mercaptopnicotinic acid; TGA, thioglycolic acid; PAA, polyacrylamide; S-chitosan, succinyl chitosan; SOD, superoxide dismutase; ALG, alginate; PGL, plasma glucose level; FA, folic acid

PLGA NPs. The oral bioavailability of delivered conjugate-loaded NPs, relative to s.c. injected solution of Ins was  $17.98 \pm 5.61\%$ , 2-fold higher over native Ins-loaded NPs. CS-based NCs conjugated with SAR6EW, a novel CPP, are prepared and evaluated by Li et al.<sup>122</sup>. The SAR6EW/CS/Ins-NPs displayed sufficient hypoglycemic effect with no significant toxicity in diabetic rats and induced a significantly higher internalization of Ins *via* clathrin- and caveolae-mediated endocytosis.

NPs decorated with specific ligand are expected to generate better binding with the epithelium and enhance the oral bioavailability. L-Valine is a target ligand distributed all over the small intestine. Li et al.<sup>83</sup> evaluated the CS-based NCs modified by L-valine and phenylboronic acid (a glucose-responsive unit). Results showed a corresponding bioavailability of  $7.55 \pm 1.32\%$  after oral administration. CSKSSDYQC (CSK) peptide has been identified to specifically recognize goblet cells, the second large cell population on epithelium. Zhang et al.<sup>84</sup> developed Ins-loaded dodecylamine-graft-g-polyglutamic acid (PGA-g-DA) micelles coated in CSK peptide-conjugated TMC. The NPs exhibited excellent hypoglycemic effect following oral administration with a relative bioavailability of 7.05%, 1.2-fold higher than that of unmodified NPs and the total decrease of PGL was 1.19-fold higher than unmodified NPs. AT-1002 is a hexamer peptide derived from zonula occludens toxin (ZOT), which has been shown to open the TJs reversibly and enhance the absorption of peptides across the epithelium. Lee et al.<sup>85</sup> developed AT-1002 peptide-CS dual ligand functionalized pluronic-based NCs for oral delivery of Ins. Results revealed that the penetration of FITC-labeled Ins-loaded dual ligand NCs across the Caco-2 cell monolayer was nearly 7%, 1.75-fold higher than single ligand conjugated NCs. *In vivo* experiment showed that the relative bioavailability of Ins-loaded dual ligand functionalized NCs significantly increased almost 10%, 6-fold higher than that of single ligand functionalized NCs. What's more, intracellular lysosomal degradation is detrimental to transepithelial transport of peptides/proteins, which cannot be overstated in the study of oral delivery. Apical sodium-dependent bile acid transporter (ASBT)<sup>123,124</sup> is different from the common receptor-mediated transport such as transferrin, vitamin B12 and lectin receptor-mediated pathways, which not only deal with the apical membrane barrier but also responsible for the intracellular trafficking and basolateral release<sup>125</sup>. SDC-conjugated CS NPs (DNPs) were synthesized by Fan et al.<sup>78</sup> and loaded with Ins. They focused on exploring the mechanism of functional NPs exploiting the bile acid pathway to overcome multiple barriers of the intestinal epithelium through CLSM, intravital two-photon microscopy and other techniques. The apical membrane was overcome through ASBT-mediated endocytosis. Moreover, DNPs escaped from the endolysosome to avoid lysosomal degradation of Ins by bonding with ileal bile acid-binding protein (IBABP) in cytoplasmic trafficking. Eventually, Ins were excreted from the basolateral membrane. Results showed that the relative bioavailability of enteric-coated DNPs was 15.9%, 2.2-fold higher than NPs without SDC. A major limitation impeding the oral delivery of NPs apart from permeating rate is the elimination of NPs by the mononuclear phagocyte system (MPS)<sup>126</sup>. Sarmiento et al.<sup>127</sup> investigated the ability of CS-coated SLNs to survive phagocytosis by the MPS after intestinal uptake using RAW 264.7 macrophage cell line. Results showed that this system demonstrated potential ability to prolong the half-life of Ins in blood and provided stealth properties by MPS after intestinal uptake. As folate receptor is significantly expressed on epithelial cells, macromolecules conjugated with folic acid (FA) can enhance their

uptake and targeting abilities. PLGA- and FA-modified CS were fabricated *via* electrostatic self-assembly method by Xu et al.<sup>128</sup>. The relative bioavailability of orally delivered Ins-loaded PLGA/FA-CS is 7.22%, which is 2.76-fold higher than that of Ins solution.

However, CS is inadequate for opening TJs in neutral pH environments, which limits its potential use as a PE only in the duodenum section. In addition, CS is only dissolved in acid solutions and has limited mucoadhesive abilities. A series of CS derivatives such as TMC, *O*- and *N*-carboxymethyl CS, *N*-methylene phosphonic CS, carbohydrate branched CS and alkylated CS are synthesized to solve these problems. Many researches have been done on TMC, which is soluble in a wide range of pH in aqueous solutions so that it could carry peptides in different organs regardless of the pH changes. CS and its derivatives such as TMC enhance the absorption of NPs *via* paracellular way by opening TJs. Omid et al.<sup>82</sup> indicated that Glycyl-glycine (GG)- and alanylalanine (AA)-conjugated TMC NPs showed enhanced 2.5–3.3-fold permeability of Ins in Caco-2 cell line than unmodified TMC NPs and demonstrated increased relative bioavailability of 17.19% and 15.46% separately compared with TMC NPs (14.15%). This enhanced absorption is explained by the presence of proton-coupled oligopeptide transporters PepT1 and PepT2 that could actively transport di/tri-peptides like GG and AA in the brush border of membrane of the small intestine. CS–6-mercaptopicolonic acid (MNA) is a thiolated CS with strong mucoadhesive properties and a pH-independent reactivity. Millottl et al.<sup>129</sup> evaluated *in vivo* the potential of CS–6-MNA for oral delivery of Ins. Results showed that CS–6-MNA tablets were at least 84-fold stronger mucoadhesive than unmodified ones. The relative bioavailability of thiolated formulations ( $M=20$  kDa) was 15.3%, 4.79-fold higher compared with non-thiolated ones, while thiolated CS of 400 kDa mass was 12.8%, 21.3-fold higher compared with non-thiolated ones. However, unless sealed under inert conditions, thiomers are prone to thiol oxidation at physiological pH<sup>130</sup>. The protection of thiol groups on the thiomers prevents an early oxidation before contacting with mucosa. Dünnhaupt et al.<sup>29</sup> prepared sulfhydryl-protected thiolated CS for oral delivery of antide. They utilized thioglycolic acid (TGA) as sulfhydryl ligand protected by the thiolated aromatic residue 6-MNA. The permeation enhancing effect of sulfhydryl-protected CS was enhanced approximately 1.2-fold than its corresponding thiomers and 2.8-fold compared to unmodified ones. Oral administration of antide incorporated TGA–MNA matrix tablets reached a relative bioavailability of 10.9%. Suksamran et al.<sup>19</sup> successfully synthesized *N*-(4-*N,N*-dimethylaminocinnamyl) CS (TM<sub>65</sub>CM<sub>50</sub>CS) as a surface coating for ovalbumin (OVA)-loaded calcium-alginate and calcium-alginate-yam microparticles, which exhibited the greatest immune responses compared with other modified CS. Although TMC-based NPs have been demonstrated to facilitate the paracellular transport of peptides across the epithelial barriers, the trapping and clearance of these NPs by the mucus layer was often overlooked. Different from other commonly used hydrophilic “mucus-inert” materials like PEG, the physicochemical properties of *N*-(2-hydroxypropyl) methacrylamide copolymer (pHPMA) can be easily tuned by manipulating the monomers. Liu et al.<sup>131</sup> designed NPs composed of Ins-loaded TMC-based polyelectrolyte complex core, and a dissociable coating of pHPMA to overcome the epithelial barriers. Results revealed that the outer pHPMA gradually dissociated from the TMC-based NP core as the NPs permeated through mucus using CLSM. At the dose of 50 IU/kg, these NPs exhibited a relative bioavailability of 8.56%, 2.8-fold higher than that of uncoated NPs.

### 3.2. Other polysaccharide-based systems

Dextran (DEX), a complex branched glucan, is consisted of chains with extensive lengths (3–2000 kDa). Soudry-Kochavi et al.<sup>32</sup> markedly improved the oral relative bioavailability of exendin-4 to 77% compared to a s.c. injection of Byetta<sup>TM</sup>. He and coworkers designed a nano-in-micro encapsulation delivery system, in which the inside nano-systems are a mixture of bovine serum albumin (BSA) and DEX NPs cross-linked with sodium trimetaphosphate (STMP) and the micro-systems are composed of an appropriate ratio of Eudragit<sup>®</sup> L100-55 (Eudragit L) and hydroxypropylmethylcellulose (HPMC) for additional protection. They hypothesized that the significantly improved oral absorption is due to DEX that increased lymphatic uptake and circumvented the first-pass effect. Heparin is a negatively charged biomolecular material mainly used as a natural anticoagulant. Park et al.<sup>77</sup> designed Pt nanocomplex-loaded heparin-SDC NPs with size of  $150.8 \pm 16.5$  nm and zeta potential of  $-29.1 \pm 3.9$  mV. They showed that the orally administered NPs were absorbed by ASBT in the epithelium of ileum, which could be applied for delivering peptides avoiding accumulative problems. Recently, PEG is questioned by inducing an immune response in human body, particularly when given repeatedly. Polysialic acid (PSA), a highly hydrophilic polysaccharide primarily composed of  $\alpha$ -2,8-linked 5-*N*-glycolyneuraminic acid, could be used as a suitable alternate of PEG as an endogenous substance. The PSA-based carrier systems are non-immunogenic and can be used to extend the half-lives similar to PEG-conjugates<sup>132,133</sup>. Wu et al.<sup>134</sup> modified the uricase to obtain the PSA-PEG-uricase conjugates, which exhibited lower immunogenicity and stronger water absorbency. Thwala et al.<sup>135</sup> indicated that coating the nanosystem with PSA improved its stability and mucosal penetration ability. They designed double layer PSA-Pt NCs. The formulations, administered intra-jejunal to healthy rats resulted in a moderate reduction of PGL (20% reduction) and lasted for 4 h.

Alginates (ALG) extracted from brown seaweed are natural water-soluble linear polysaccharides composed of  $\alpha$ -L-guluronic acids and  $\beta$ -D-mannuronic acids. They are anionic compounds featured by the capability to form hydrogels in the presence of divalent cations such as  $\text{Ca}^{2+}$  and have significant advantages in oral delivery for their pH sensitivity and low cost<sup>44</sup>. Lee et al.<sup>28</sup> encapsulated superoxide dismutase (SOD) in zein-ALG NPs (ZAN) *via* a phase separation method. Carboxyl groups in ALG are protonated at low pH and the ZAN swell slightly in the stomach. ZAN (*w/w* 200:40) releases  $90.8 \pm 1.2\%$  of encapsulated SOD at pH 7.4 in 2 h, while only  $11.4 \pm 0.4\%$  of SOD was released at pH 1.3. Mukhopadhyay et al.<sup>136</sup> developed Ins-loaded CS/ALG core-shell NPs with an average particle size of 100–200 nm. After oral administration, a significant reduction of PGL with a sustained effect at least 9 h and a relative bioavailability of nearly 8.11% were detected. The fact that some virus having hydrophilic and neutral surface composed of both positive and negative charges less hindered in mucus offers a new idea for designing mucus-penetrating NPs. Zhang et al.<sup>137</sup> designed an intestinal mucus-penetrating core-shell nanocomplex through self-assembly between positive Ins-loaded CS/TPP with negative ALG. These nanocomplexes with negative ALG coating were confirmed to have 1.6–2.5 times higher mucus penetration abilities than CS NPs. However, compared to PEGylated NPs which have 20-fold mucus penetrating ability than uncoated NPs, ALG-coated nanocomplexes needs further improving. Lopes et al.<sup>138</sup> formulated Ins-loaded ALG/DEX NPs and dual-coated with CS and ALB, in which

ALB provided electrostatic stabilization and enhanced dissolution rate of Ins from NPs. It was demonstrated to transport actively by clathrin-mediated endocytosis. Eldin et al.<sup>23</sup> synthesized pH-sensitive L-arginine grafted alginate (Arg-g-Alg) hydrogel beads and utilized it as a new carrier for BSA. Arg-g-Alg showed sufficient release profile with about 300% in acidic media compared to pure alginate hydrogel beads. However, attention should be poured into the process of introducing negatively charged shell into drug loaded core because competitive interactions among different materials may lead to a decrease in drug loading.

Cellulose is one of the most widely used natural substances and commercial biopolymers. Microcrystalline cellulose and cellulose derivatives, such as HPMC, hydroxypropyl cellulose (HPC), hydroxyethyl cellulose (HEC), and carboxymethyl cellulose (CMC) are recognized as the natural materials with good tolerance in body and often used as pH-sensitive coating materials to protect encapsulated peptides<sup>139</sup>. Song et al.<sup>139</sup> prepared the oppositely charged CMC and quaternized cellulose NPs by changing the ratio of anionic-to-cationic polymers and selected two proteins, lysozyme (*pI* 11.4) and BSA (*pI* 4.8) with opposite charges. Results revealed that positively charged NPs were more efficiently internalized. However, the negatively charged NPs may be more appropriately applied in delivering drugs such as Ins, which needs the longer half-life. An oral multiple-unit formulation for colonic release of Ins was proposed by Maroni et al.<sup>51</sup>. The system comprises an immediate-release minitab core containing the protein and SGC coated by HPMC as a swellable internal layer. Oral administration of the novel formulation to diabetic rats elicited a peak in PGL after 6 h associated with a sharp decrease in the PGL. The relative bioavailability of such formulation was 2.2-fold higher than that of uncoated ones. Makhlof et al.<sup>140</sup> formulated CS NPs with hydroxypropyl methylcellulose phthalate (HPMCP,  $\text{pK}_a$  5.2) as a pH-sensitive polymer. Fluorescently-labeled CS/HPMCP NPs showed 2–4 times improvement in the intestinal mucoadhesion and penetration compared to CS/TPP NPs. Following oral administration, CS/HPMCP NPs with a relative bioavailability of  $8.47 \pm 1.59\%$  increased the hypoglycemic effect by more than 2.8-fold compared to Ins-loaded CS/TPP NPs. In addition, Singh et al.<sup>141</sup> developed an ileum-targeted protein delivery system using HPMCP. Initially, they attuned pH-sensitive property of HPMCP for controlled dissolution at ileum pH ( $\geq 7.4$ ) by thiolation, which prevented the early release of protein in acidic pH in stomach and duodenum but at ileal pH in a controlled manner. Wu et al.<sup>142</sup> developed a two-stage delivery system composed of PLGA/ Eudragit<sup>®</sup> RS NPs coated with pH-sensitive hydroxypropyl methylcellulose phthalate (HP55,  $\text{pK}_a$  5.5) for the oral delivery of Ins, in which HP55 was designed to overcome the first barrier. PLGA/RS NPs, as the second stage, adhered to the intestine mucosa and improved the absorption of Ins. The hypoglycemic effect and relative bioavailability of the enteric-coated capsule were 32.9% and 9.2%, respectively. For further insight, Wang et al.<sup>143</sup> investigated the structure–function relationship of PLGA/HP55 NPs in different conditions by dissipative particle dynamics simulations (DPD). It can be seen that all polymeric molecules formed spherical core-shell NPs with PVA molecules as a stabilizer adsorbed on the PLGA/HP55 matrix.

## 4. Inorganic particles

Some of the inorganic NCs have been successfully applied in oral delivery of therapeutic peptides/proteins, gold NPs (Au NPs)<sup>145,146</sup>, selenium NPs (Se NPs)<sup>41</sup>, silica NPs (Si NPs)<sup>43,147,148</sup>, alumina<sup>149</sup>,

**Table 7** Summary of inorganic particles in oral delivery of therapeutic peptides/proteins.

Formulation composition	Model drug	Main transport mechanisms	Characterization (size, ZP, EE)	PK		PD	Ref.
				Dose	F (%)		
NiMOS-loaded HNTs	Albuimn	N/A	Size: 215.3 ± 2.5 nm; EE: 63.16 ± 4.66%	N/A	N/A	N/A	25
SiNPs-PEG	Ins	N/A	Size: 493.7 ± 89.10 nm; ZP: -15.2 ± 0.0 mV; EE: 85.4%	N/A	N/A	N/A	43
A bubble carrier system loading DTPA, SBC, SDS and Ins	Ins	Transcellular way and paracellular way in free-form insulin	Size: 150 nm	30 IU/kg	21.7 ± 1.7	A steady decrease of PGL for over 10 h with maximum decrease of 50% 4–5 h	61
Chondroitin sulfate capped AuNPs	Ins	CD44 receptor-mediated endocytosis	Size: 122.90 ± 7.12 nm; ZP: -33.69 ± 3.39 mV; EE: 90.19 ± 3.42%	N/A	N/A	50% decrease of PGL in 4 h	87
Montmorillonite coated with TiO <sub>2</sub>	Ins	N/A	Size: 50 nm; ZP: -54.5 mV	N/A	N/A	N/A	150
SeNPs	Ins	Clathrin-dependent endocytosis	Size: 100–200 nm; ZP: 25 mV; EE: 95.97%	50 IU/kg	9.15	50% decrease of initial PGL maintaining for 10 h	152
Silica coating HP55	Ins	N/A	Size: 50 nm; EE: 27.4%	N/A	N/A	PGL maintained from 40% to 70% for a period of 2–7 h.	156
Ins/ZrP coated with TiO <sub>2</sub>	Ins	N/A	Size: 364.2 ± 53.9 nm; ZP: 27.3 ± 2.4 mV	N/A	N/A	N/A	159

ZP, zeta potential; EE, encapsulation efficiency; F, relative bioavailability; PGL, plasma glucose levels; NiMOS, nanotubes-in-microgel oral system; HNTs, halloysite nanotubes

TiO<sub>2</sub><sup>150</sup>, zirconium phosphate (ZrP)<sup>145,151</sup>, for instance. In comparison with organic matrices, these materials are born with noticeable stabilities in acidic and enzymatic environment. Summary of inorganic particles applied in oral delivery of therapeutic peptides/proteins are showed in Table 7.

Chondroitin sulfate capped Au NPs/Ins with around 120 nm were prepared by Cho et al.<sup>87</sup>. Chondroitin sulfate was used as a stabilizing agent for synthesis of Au NPs. The mean concentration of Ins in plasma at 2 h after oral treatment was 6.61-fold enhanced than that of Ins solution. It was shown that Se has similiar hypoglycemic effect with Ins by improving pancreatic islet function and glucose utilization in latest research<sup>41</sup>. Deng et al.<sup>152</sup> fabricated Ins-loaded Se NPs around 120 nm by ionic cross-linking/*in situ* reduction technique. Ins-SeNPs (50 IU/kg) resulted in a relative bioavailability of 9.15% and a decreased PGL of 50% of starting levels sustaining 10 h. Hydroxyapatite (HAP), a biocompatible and porous material with no obvious poisonous effects, might be an ideal drug carrier. Zhang et al.<sup>153</sup> prepared HAP NPs wrapped by PEG which conjugated with Ins and gallic acid (GA) and showed a downward trend of PGL after directly administered to the ileum.

Si NPs with large specific surface area and high porosity are promising candidates for the excellent biocompatibility and biodegradability<sup>154</sup>. What's more, Si NPs possess residual silanol groups (Si-OH) at surface that can be functionalized by different organic groups<sup>155</sup>. Zhao et al.<sup>156</sup> prepared Ins-loaded Si NPs coated with HP55. *In vivo* evaluation showed a significant hypoglycemic effect that was maintained from 40% to 70% in

2–7 h. However, Andreani et al.<sup>43,157</sup> produced PEG-coated Si NPs for oral administration of Ins. Si NPs-PEG<sub>20,000</sub> showed a faster diffusion followed by Si NPs-PEG<sub>6000</sub> and Si NPs. They further reported the development of Ins-Si NPs coated with mucoadhesive polymers such as CS, ALG or PEG of low and high MW. Si NPs coated with ALG or CS showed higher contact with mucin compared to non-coated Si NPs and Si NPs-PEG. Si could prevent coalescence of emulsion droplets by forming stable networks and a rigid protective barrier. A hybrid nanocapsule using liposomes as template for the deposition of Si NPs or CS was developed by Mohanraj et al.<sup>158</sup>. The results exhibited increased EE up to 70% and controlled release.

In addition, hybrid carriers coated by inorganic materials are applied to achieve controlled release. Safari et al.<sup>159</sup> synthesized a series of Ins/ZrP composites coated with TiO<sub>2</sub> by sol-gel means. The TiO<sub>2</sub>-coated composites prolonged drug release and enhanced EE considerably compared to the Ins/ZrP composites. Similarly, Kamari et al.<sup>150</sup> successfully prepared hybrid nanocomposites composed of montmorillonite (Mt)/Ins/TiO<sub>2</sub>. Mt has a large surface area and a high capacity of cation exchange. Results revealed that nanocomposites without and with TiO<sub>2</sub> coating released cargos after 60 min and 22 h in pH 7.4, respectively. In addition, microencapsulation approaches, such as prilling protein into microspheres, may protect it from enzymatic degradation in GIT. Kruif et al.<sup>25</sup> demonstrated a nanotubes-in-microgel oral system prepared by prilling, a mild process embedding BSA-loaded halloysite nanotubes, which demonstrated a higher enzymatic protection than pure nanotube.

## 5. Synthetic macromolecular polymer delivery systems

A new range of biodegradable polymeric NPs that are easily functionalized have been synthesized and recently applied in oral delivery of therapeutic proteins/peptides in order to enhance their stability and realize controlled release<sup>160</sup>. Summary of synthetic macromolecular polymers applied in oral delivery of therapeutic peptides/proteins are shown in Table 8.

Mucosal layer acts as a protective barrier can trap foreign particulates and clear them subsequently, which consequently diminished the possibilities for NPs to traverse the absorptive membrane of the intestine. PEG would render more hydrophilic the NPs to pass through the mucus and prevents from aggregation due to its steric hinderance effect. Inchaurreaga and coworkers<sup>161</sup> evaluated *in vivo* the mucus-penetrating abilities of PEG-coated poly(anhydride) NPs, which was clearly influenced by both the MW and surface density of coated PEG. The mucus-penetrating abilities were higher for PEG<sub>2000</sub> or PEG<sub>6000</sub> coated NPs than PEG<sub>10,000</sub> and lower for excessive densities of coated PEG. However, a dilemma occurs when selecting proper materials between high mucus permeation and high epithelial transshipment. LMWP (VSRRRRRRGGRRRR), composed of 10 arginine residues, could function as a CPP to achieve effective intracellular transport<sup>162</sup>. Shan et al.<sup>163</sup> demonstrated that the NPs co-loaded with CPP as a core and then coating dissociable pHPMA could successfully solve the dilemma. The NPs exhibited 20-fold higher absorption than free Ins on epithelial cells that secrete mucus. They further indicated that organelles including endoplasmic reticulum (ER), Golgi apparatus and lysosome were all participants in the intracellular trafficking of NPs. He et al.<sup>45</sup> developed monomeric Ins/LMWP conjugates (w/w, 1:1) by using succinimidyl-[(N-maleimidopropionamido)-polyethyleneglycol] ester as an intermediate cross-linker. It is demonstrated that transport of the conjugates across the mucosal monolayer was almost 5-fold higher than free Ins. The *in vivo* bioavailability of the *in situ* loop administered conjugates was 7.08%, 3.9-fold higher than physical mixture. It has been reported that Zn<sup>2+</sup> improves the thermal stability of cargos by forming Zn<sup>2+</sup>-imidazole coordination complexes *via* modulating Zn<sup>2+</sup> at the active site of proteins. Zhang et al.<sup>36</sup> used PEG-PLGA as the forming polymer to orally deliver LMWP-exenatide-Zn<sup>2+</sup> complexes. The relative bioavailability of LMWP-exenatide-Zn<sup>2+</sup> NPs was augmented by 1.74-fold compared to LMWP free NPs. Additionally, the AUC of exenatide-Zn<sup>2+</sup> NPs was 3.27-fold higher than NPs contained no Zn<sup>2+</sup>, which confirmed the function of Zn<sup>2+</sup> in improving the biological activity of exenatide.

PLGA is a promising drug delivery vehicle as it has been approved by the US Food and Drug Administration for applying in biomedicine. The instability of Ins-loaded PLGA microparticles was reported due to deamidation. To incorporate antacids could help overcome such problems by preventing aggregation and increasing pH of microclimate. Therefore, Sharma et al.<sup>53</sup> developed antacid-Ins co-encapsulated PLGA NPs for oral delivery, the oral bioavailability of which augmented 6-fold compared with native Ins in healthy rats. The hydrophobic nature of PLGA hampers its effective load of hydrophilic drugs. Hence, amphiphilic block copolymers are designed to increase the EE of hydrophilic proteins. Hosseininasab et al.<sup>47</sup> synthesized Ins-loaded PLGA-PEG copolymer NPs using the double-emulsion method (w/o/w), in which PEG<sub>2000</sub> showed higher EE (62.3 ± 5.6%) than PEG<sub>4000</sub>. Although PEG has been widely used as a hydrophilic segment of diblock copolymers, it might lead a protein-repelling effect. García-Díaz et al.<sup>164</sup> incorporated premixing amphiphilic lipids-Ins into PLGA NPs, resulting in a

significantly enhanced EE of 90% than 24% in the absence of lipids. Besides, DEX is peptides-friendly to use in block copolymers as a hydrophilic segment. Alibolandi et al.<sup>42</sup> synthesized Ins-encapsulated DEX-PLGA amphiphilic copolymers, which showed an average EE more than 90% with sustained release of Ins at pH 7.4. The polymeric lipid NPs combined properties of both polymeric and liposomes realized a relative bioavailability of 9.77%. Ma et al.<sup>20</sup> reported ulex europaeus agglutinin-1 (UEA-1) conjugated PLGA-lipid NPs to orally deliver OVA, which contained an M-cell selective molecular signature toll-like receptor (TLR)-agonist monophosphoryl lipid (MPL) to effectively transport through M-cells.

Recent studies have revealed that NPs coated with hydrophilic polymers exhibit less adhesion to mucus layer. To further improve the mucus penetration of NPs, Li et al.<sup>50</sup> designed core shell corona nanolipoparticles (CSC) containing CS NPs as core, pluronic F127-lipid vesicles as shell and polyethylene oxide (PEO) as a corona. The cellular level of Ins after CSC treatment was 10-fold higher compared to CS NPs, exhibiting significantly higher efficiency of mucosal penetration. Studies in diabetic rats showed 2.5 times the hypoglycemic effects of CSC and 2.1-fold times the relative bioavailability than CS NPs. Salvioni et al.<sup>88</sup> applied a three-layer colonic system to prepare polyethylene imine (PEI) coated Ins-DEX NPs. The three-layer release technology platform was consisting of a flexible film composed of a neutral polymethacrylate Eudragit<sup>®</sup> NE and sodium starch glycolate Explotab<sup>®</sup>, applied to a HPMC coating of reduced thickness in order to delay the drug liberation. Compared with s.c. Ins that led to 25% of the starting level of glucose concentration at 1 h post-treatment, the PGL in rats administered with the particles gradually decreased and remained at 45%.

Mucus is incessantly secreted, shed and digested as a dynamic gel. In many cases, the mucus clears the drug carriers before loaded cargos reaching the underlying cells and entering the blood circulation. A promising technique occurred to reach the epithelial layer by cleavage of mucoglycoprotein substructures on mucus through proteases like papain (PAP) and bromelain (BRO). Poly (acrylic) acid with weak mucoadhesion bears carboxylic groups that enzymes can be conjugated with. Müller et al.<sup>165</sup> prepared PAP-grafted PAA NPs *via* ionic gelation. Permeation studies revealed that PAP conjugated particles diffused 3.0-fold higher across mucosal layer than unmodified ones. PAP and BRO were separately conjugated to PAA by Pereira de Sousa et al.<sup>166</sup> BRO modified NPs exhibited higher permeating abilities by altering the structure of mucosal layer compared to PAP conjugated ones. Koetting et al.<sup>11,13</sup> synthesized pH-responsive hydrogels composed of itaconic acid (IA) copolymerized with *N*-vinylpyrrolidone (NVP) to orally deliver therapeutic proteins with high pI. NVP was chosen to be a hydrogen-bond acceptor as it offers enhanced protection for proteins. Results showed that these hydrogels rapidly and completely release sCT within 1 h in simulated intestinal fluid (SIF) while undetectable release in simulated gastric fluid (SGF). Arginine-rich polymers have received increasing attentions in oral delivery for their higher efficiency in crossing epithelial cells than the other polycationic polymers. He et al.<sup>46</sup> synthesized a new arginine-based poly(ester amide) (Arg-PEA) combined with PEA-COOH for the protection of Ins. PEA is a biodegradable polymer with good mechanical and thermal properties. *In vivo* test revealed that the PGL can be effectively controlled in 10 h, and the oral bioavailability was 5.89 ± 1.84% in healthy rats.

Ligand-functionalization can increase the affinities of NPs with targeted cells. Butyrate functionalization PEG (Bu-PEG) NPs,

**Table 8** Summary of synthetic macromolecular polymers in oral delivery of therapeutic peptides/proteins.

Formulation composition	Model drug	Main transport mechanisms	Characterization (size, ZP, EE)	PK		PD	Ref.
				Dose	F (%)		
mPEG- <i>g</i> -AA	sCT	Transcellular way	Size: 72.1 ± 0.5 nm; EE: 72.8%	N/A	N/A	77.7% decrease of serum calcium level was observed within 1 h and last 7 h	12
LMWP-PEG-PLGA	Exendin-4	Transcellular way	Size: 114.4 ± 10.5 nm; ZP: 2.5 ± 0.2 mV; EE: 71.3 ± 4.3%	100 µg/kg	7.44	55% decrease of PGL in 24 h	36
Dextran <sub>5000</sub> - <i>b</i> -PLGA <sub>13000</sub> polymersome	Ins	Lectin-like protein receptors (not confirmed)	Size: 139.2 ± 12.23 nm; EE: 90.42 ± 1.39%	100 IU/kg	9.77	75% decrease of PGL in 12 h	42
INS-PEG-LMWP conjugate	Ins	N/A	N/A	50 IU/kg	7.08	The BGL dropped considerably by 70% in 10 h	45
PEA-COOH/Arg-PEA microspheres	Ins	N/A	Size: 13.4 ± 5.8 µm; EE: 80.2 ± 1.3%	50 IU/kg	5.89 ± 1.84	50% decrease of PGL in 10 h	46
CS/pluronic F127-lipid vesicles/PEO core shell corona nanolipoparticles	Ins	N/A	Size: 195.3 ± 32.9 nm; ZP: 4.3 ± 5.4 mV; EE: 76.6 ± 5.8%	50 IU/kg	7.8	50% decrease of PGL in 12 h	50
Antacid (magnesium hydroxide or zinc carbonate)-Ins co-encapsulated PLGA NPs	Ins	Via the M cells of the Peyer's patches (not confirmed)	Size: ~136–143 nm; EE: 81%–85%	120 IU/kg	1.2	74% decrease of PGL in 30 h	53
Bu-PEG NPs	Ins	MCT1-mediated endocytosis	Size: 90.8 ± 1.73 nm; ZP: -9.89 ± 0.11 mV; EE: 57.47 ± 0.03%	50 IU/kg	9.28	58.8% decrease of PGL after 4 h	86
Ins-LMWP conjugates loaded TMC-coated PLGA nanoparticles	Ins	Paracellular way and clathrin-dependent endocytosis and adsorptive endocytosis.	Size: 2 53.8 ± 6.4 nm; ZP: 47.5 ± 3.8 mV; EE: 49.3 ± 2.1%	20 IU/kg	17.98 ± 5.61	50% decrease of PGL in 9 h	121
Insulin/CPP NCs coated pHPMA	Ins	Paracellular way	Size: 177.3 ± 15.2 nm; ZP: -10 mV; EE: 94.9 ± 1.1%	75 IU/kg	3.02 ± 0.66	50% decrease of PGL in 10 h	163
ConA-PEG-PLGA	Ins	Lectin-receptor mediated transport	Size: 196.3 ± 4.5 nm; ZP: -25.6 ± 1.68 mV; EE: 44.6 ± 3.5%	N/A	N/A	60% decrease of PGL in 20 h	167
C12(Chol)-r8-Ins loaded diblock PEG-PGA NPs	Ins	N/A	Size: 236 ± 27 nm (225 ± 10 nm); ZP: 2 ± 2 mV (2 ± 3 mV); EE: 99 ± 0% ; (92 ± 9%)	N/A	N/A	There are not statistically significant differences between the Ins and the ENCP formulation	168

ZP, zeta potential; EE, encapsulation efficiency; F, relative bioavailability; PGL, plasma glucose levels; LMWP, low molecular weight protamine; PEG, polyethylene glycol; PLGA, poly(lactic-co-glycolic acid); PGA, poly (glutamic acid); pHPMA, *N*-(2-hydroxypropyl) methacrylamide copolymer; PGA-*g*-DA, dodecylamine-graft-*g*-polyglutamic acid; PEO, polyethylene oxide; PGL, plasma glucose level; Bu-PEG, butyrate-conjugated PEG; MCT1, monocarboxylate transporter 1; mPEG-*g*-AA, mPEG grafted alginate acid; Con A, concanavalin A; PEA, poly(ester amide); ARG, arginine; DOCA, deoxycholic acid; TMC, *N*-trimethyl chitosan.



established by Wu et al.<sup>86</sup> generated a stronger hypoglycemic effect in diabetic rats and a relative bioavailability of 9.28%, which increased 2.87-fold than bare PEG NPs. Enhanced cellular uptake was achieved *via* specific interaction between butyrate and the monocarboxylate transporter (MCT) on cell membranes. Li et al.<sup>12</sup> demonstrated that the mPEG grafted alginate micelles with size of 72 nm could significantly improve ( $P < 0.001$ ) the oral absorption of sCT by transcellular way. Lectins (concanavalin A) are proteins or glycoproteins that specifically recognize carbohydrate moieties and trigger active vesicular transport by endocytosis. Concanavalin A anchored PEG-PLGA diblock copolymers were synthesized by Sharma et al.<sup>167</sup>. The established system showed a delayed response (2–4 h) in the reduction of PGL within an acceptable range. Samstein et al.<sup>79</sup> hypothesized that bile salts could be used to enhance the bioavailability of PLGA NPs by protection and elevated absorption. Oral administration of Ins loaded PLGA NPs to mice, using a SDC emulsion, produced sustained levels of the PGL over 24–48 h with a relative bioavailability of 1.81%.

Although numerous oral protein/peptide delivery systems using synthetic polymers as carriers have been established, these polymers still face considerable challenges in toxicological evaluation, biocompatibility, and biodegradability.

## 6. Conclusions and future perspectives

Obviously, the oral bioavailabilities of therapeutic proteins/peptides are seriously hampered by the atrocious conditions in GIT. It is increasingly recognized that in order to overcome these physiological barriers for successful delivery, drug delivery systems embracing protection ability for drug carriers, modified release behavior for cargos, enhanced stability by PIs, elevated uptake by PEs, and escape ability from MPS are somehow required. The multifunctional materials utilized to modify the surface of NPs for oral delivery can produce “smart” NCs such as pH-triggered and targeted release systems. Although a considerable number of formulated multifunctional delivery systems have shown the potential for oral delivery of therapeutic proteins/peptides, further issues concerning the safety and side effect, EE and LC of drug loaded carriers, typicality of *in vitro* models, reproducibility of fabrication technique, feasibility of storage condition, and reproducible therapeutic effect in human need to be addressed. What's more, the influence of anesthetics and sampling methods for evaluating oral drug delivery systems of peptides/proteins cannot be overstated<sup>169</sup>. At present, lack of information being available about the detailed absorption mechanism of established delivery systems *in vivo* is a major barrier to progress in further study. More mechanism studies are needed to shed new insights on the details of intestinal absorption of NPs to realize the rational design of NPs and enhanced oral bioavailability<sup>170</sup>. After being endocytosed, NCs interact with different organelles, including endosomes, lysosomes, ER, and the Golgi apparatus, and transport *via* diverse routes, such as the endolysosomal, ER/Golgi, and cytoplasmic routes, resulting in totally different destinies. Whether these interactions of NCs with organelles are beneficial to the oral delivery of peptides/proteins remains to be investigated<sup>171</sup>. In particular, intracellular lysosomal degradation is detrimental to transepithelial transport of peptides/proteins, which should be paid real attention to in the field of oral peptides/protein delivery in future study. All in all, these new delivery systems paved a new way in oral delivery of therapeutic peptides /proteins.

## Acknowledgments

This work was financially supported by the CAMS Innovation Fund for Medical Sciences (CAMS-2017-12M-1-011, China), National Natural Science Foundation of China (81373342), the Fundamental Research Funds for the Central Universities and PUMC Youth Fund (2017350003, China) and PUMC Basic Fund (2018PT35002, China).

## References

1. Aguirre TA, Teijeiro-Osorio D, Rosa M, Coulter IS, Alonso MJ, Brayden DJ. Current status of selected oral peptide technologies in advanced preclinical development and in clinical trials. *Adv Drug Deliv Rev* 2016;**106**:223–41.
2. Malhaire H, Gimel JC, Roger E, Benoit JP, Lagarce F. How to design the surface of peptide-loaded nanoparticles for efficient oral bioavailability?. *Adv Drug Deliv Rev* 2016;**106**:320–36.
3. Rekha MR, Sharma CP. Oral delivery of therapeutic protein/peptide for diabetes—future perspectives. *Int J Pharm* 2013;**440**:48–62.
4. Brayden DJ, Alonso MJ. Oral delivery of peptides: opportunities and issues for translation. *Adv Drug Deliv Rev* 2016;**106**:193–5.
5. Gaowa A, Horibe T, Kohno M, Kawakami K. Bile acid as an effective absorption enhancer for oral delivery of epidermal growth factor receptor-targeted hybrid peptide. *J Pharm Sci* 2018;**107**:1322–9.
6. Uhl P, Pantze S, Storck P, Parmentier J, Witzigmann D, Hofhaus G, et al. Oral delivery of vancomycin by tetraether lipid liposomes. *Eur J Pharm Sci* 2017;**108**:111–8.
7. Uhl P, Helm F, Hofhaus G, Brings S, Kaufman C, Leotta K, et al. A liposomal formulation for the oral application of the investigational hepatitis B drug myrcludex B. *Eur J Pharm Biopharm* 2016;**103**:159–66.
8. Parmentier J, Hofhaus G, Thomas S, Cuesta LC, Gropp F, Schroder R, et al. Improved oral bioavailability of human growth hormone by a combination of liposomes containing bio-enhancers and tetraether lipids and omeprazole. *J Pharm Sci* 2014;**103**:3985–93.
9. Parmentier J, Thewes B, Gropp F, Fricker G. Oral peptide delivery by tetraether lipid liposomes. *Int J Pharm* 2011;**415**:150–7.
10. Bonengel S, Jelkmann M, Abdulkarim M, Gumbleton M, Reinstadler V, Oberacher H, et al. Impact of different hydrophobic ion pairs of octeotide on its oral bioavailability in pigs. *J Control Release* 2018;**273**:21–9.
11. Koetting MC, Guido JF, Gupta M, Zhang A, Peppas NA. pH-responsive and enzymatically-responsive hydrogel microparticles for the oral delivery of therapeutic proteins: effects of protein size, crosslinking density, and hydrogel degradation on protein delivery. *J Control Release* 2016;**221**:18–25.
12. Li N, Li XR, Zhou YX, Li WJ, Zhao Y, Ma SJ, et al. The use of polyion complex micelles to enhance the oral delivery of salmon calcitonin and transport mechanism across the intestinal epithelial barrier. *Biomaterials* 2012;**33**:8881–92.
13. Koetting MC, Peppas NA. pH-Responsive poly(itaconic acid-co-N-vinylpyrrolidone) hydrogels with reduced ionic strength loading solutions offer improved oral delivery potential for high isoelectric point-exhibiting therapeutic proteins. *Int J Pharm* 2014;**471**:83–91.
14. Gradauer K, Barthelmes J, Vonach C, Almer G, Mange H, Teubl B, et al. Liposomes coated with thiolated chitosan enhance oral peptide delivery to rats. *J Control Release* 2013;**172**:872–8.
15. Garg V, Kaur P, Singh SK, Kumar B, Bawa P, Gulati M, et al. Solid self-nanoemulsifying drug delivery systems for oral delivery of polypeptide-k: formulation, optimization, *in-vitro* and *in-vivo* anti-diabetic evaluation. *Eur J Pharm Sci* 2017;**109**:297–315.
16. Zupancic O, Rohrer J, Thanh Lam H, Griessinger JA, Bernkop-Schnurch A. Development and *in vitro* characterization of self-emulsifying drug delivery system (SEDDS) for oral opioid peptide delivery. *Drug Dev Ind Pharm* 2017;**43**:1694–702.

17. Lollo G, Gonzalez-Paredes A, Garcia-Fuentes M, Calvo P, Torres D, Alonso MJ. Polyarginine nanocapsules as a potential oral peptide delivery carrier. *J Pharm Sci* 2017;**106**:611–8.
18. Yoshida M, Kamei N, Muto K, Kunisawa J, Takayama K, Peppas NA, et al. Complexation hydrogels as potential carriers in oral vaccine delivery systems. *Eur J Pharm Biopharm* 2017;**112**:138–42.
19. Suksamran T, Ngawhirunpat T, Rojanarata T, Sajomsang W, Pitaksuteepong T, Opanasopit P. Methylated *N*-(4-*N,N*-dimethylaminocinnamyl) chitosan-coated electrospray OVA-loaded microparticles for oral vaccination. *Int J Pharm* 2013;**448**:19–27.
20. Ma T, Wang L, Yang T, Ma G, Wang S. M-cell targeted polymeric lipid nanoparticles containing a Toll-like receptor agonist to boost oral immunity. *Int J Pharm* 2014;**473**:296–303.
21. Song Y, Chen L. Effect of net surface charge on physical properties of the cellulose nanoparticles and their efficacy for oral protein delivery. *Carbohydr Polym* 2015;**121**:10–7.
22. Kowapradit J, Apirakaramwong A, Ngawhirunpat T, Rojanarata T, Sajomsang W, Opanasopit P. Methylated *N*-(4-*N,N*-dimethylaminobenzyl) chitosan coated liposomes for oral protein drug delivery. *Eur J Pharm Sci* 2012;**47**:359–66.
23. Mohy Eldin MS, Kamoun EA, Sofan MA, Elbayomi SM. L-Arginine grafted alginate hydrogel beads: a novel pH-sensitive system for specific protein delivery. *Arab J Chem* 2015;**8**:355–65.
24. Xu B, Zhang W, Chen Y, Xu Y, Wang B, Zong L. Eudragit<sup>®</sup> L100-coated mannosylated chitosan nanoparticles for oral protein vaccine delivery. *Int J Biol Macromol* 2018;**113**:534–42.
25. de Kruijff JK, Ledergerber G, Garofalo C, Fasler-Kan E, Kuentz M. On prilled nanotubes-in-microgel oral systems for protein delivery. *Eur J Pharm Biopharm* 2016;**101**:90–102.
26. Christophersen PC, Birch D, Saarinen J, Isomaki A, Nielsen HM, Yang M, et al. Investigation of protein distribution in solid lipid particles and its impact on protein release using coherent anti-stokes Raman scattering microscopy. *J Control Release* 2015;**197**:111–20.
27. Christophersen PC, Zhang L, Yang M, Nielsen HM, Mullertz A, Mu H. Solid lipid particles for oral delivery of peptide and protein drugs I—elucidating the release mechanism of lysozyme during lipolysis. *Eur J Pharm Biopharm* 2013;**85**:473–80.
28. Lee S, Kim YC, Park JH. Zein–alginate based oral drug delivery systems: protection and release of therapeutic proteins. *Int J Pharm* 2016;**515**:300–6.
29. Dunnhaupt S, Barthelmes J, Iqbal J, Perera G, Thurner CC, Friedl H, et al. *In vivo* evaluation of an oral drug delivery system for peptides based on *S*-protected thiolated chitosan. *J Control Release* 2012;**160**:477–85.
30. Park H, Cho S, Janat-Amsbury MM, Bae YH. Enhanced thermogenic program by non-viral delivery of combinatory browning genes to treat diet-induced obesity in mice. *Biomaterials* 2015;**73**:32–41.
31. Sneh-Edri H, Likhtenshtein D, Stepensky D. Intracellular targeting of PLGA nanoparticles encapsulating antigenic peptide to the endoplasmic reticulum of dendritic cells and its effect on antigen cross-presentation *in vitro*. *Mol Pharm* 2011;**8**:1266–75.
32. Soudry-Kochavi L, Naraykin N, Nassar T, Benita S. Improved oral absorption of exenatide using an original nanoencapsulation and microencapsulation approach. *J Control Release* 2015;**217**:202–10.
33. Sukyung A, In-Hyun L, Eunhye L, Hyungjun K, Yong-Chul K, Sangyong J. Oral delivery of an anti-diabetic peptide drug *via* conjugation and complexation with low molecular weight chitosan. *J Control Release* 2013;**170**:226–32.
34. Nguyen HN, Wey SP, Juang JH, Sonaje K, Ho YC, Chuang EY, et al. The glucose-lowering potential of exendin-4 orally delivered *via* a pH-sensitive nanoparticle vehicle and effects on subsequent insulin secretion *in vivo*. *Biomaterials* 2011;**32**:2673–82.
35. Kong JH, Oh EJ, Chae SY, Lee KC, Hahn SK. Long acting hyaluronate–exendin 4 conjugate for the treatment of type 2 diabetes. *Biomaterials* 2010;**31**:4121–8.
36. Zhang L, Shi Y, Song Y, Sun X, Zhang X, Sun K, et al. The use of low molecular weight protamine to enhance oral absorption of exenatide. *Int J Pharm* 2018;**547**:265–73.
37. Mengshu W, Yong Z, Bingxue S, Yanan S, Xin G, Yongge W, et al. Permeability of exendin-4-loaded chitosan nanoparticles across MDCK cell monolayers and rat small intestine. *Biol Pharm Bull* 2014;**37**:740–7.
38. Menzel C, Holzeisen T, Laffleur F, Zaichik S, Abdulkarim M, Gumbleton M, et al. *In vivo* evaluation of an oral self-emulsifying drug delivery system (SEDDS) for exenatide. *J Control Release* 2018;**277**:165–72.
39. Araujo F, Shrestha N, Shahbazi MA, Liu D, Herranz-Blanco B, Makila EM. Microfluidic assembly of a multifunctional tailorable composite system designed for site specific combined oral delivery of peptide drugs. *ACS Nano* 2015;**9**:8291–302.
40. Araujo F, Shrestha N, Gomes MJ, Herranz-Blanco B, Liu D, Hirvonen JJ, et al. *In vivo* dual-delivery of glucagon like peptide-1 (GLP-1) and dipeptidyl peptidase-4 (DPP4) inhibitor through composites prepared by microfluidics for diabetes therapy. *Nanoscale* 2016;**8**:10706–13.
41. Al-Quraishy S, Dkhil MA, Moneim AEA. Anti-hyperglycemic activity of selenium nanoparticles in streptozotocin-induced diabetic rats. *Int J Nanomed* 2015;**10**:6741–56.
42. Alibolandi M, Alabdollah F, Sadeghi F, Mohammadi M, Abnous K, Ramezani M, et al. Dextran-*b*-poly(lactide-*co*-glycolide) polymer-some for oral delivery of insulin: *in vitro* and *in vivo* evaluation. *J Control Release* 2016;**227**:58–70.
43. Andreani T, de Souza AL, Kiill CP, Lorenzon EN, Fangueiro JF, Calpena AC, et al. Preparation and characterization of PEG-coated silica nanoparticles for oral insulin delivery. *Int J Pharm* 2014;**473**:627–35.
44. Chaturvedi K, Ganguly K, Nadagouda MN, Aminabhavi TM. Polymeric hydrogels for oral insulin delivery. *J Control Release* 2013;**165**:129–38.
45. He H, Sheng J, David AE, Kwon YM, Zhang J, Huang Y, et al. The use of low molecular weight protamine chemical chimera to enhance monomeric insulin intestinal absorption. *Biomaterials* 2013;**34**:7733–43.
46. He P, Liu H, Tang Z, Deng M, Yang Y, Pang X, et al. Poly(ester amide) blend microspheres for oral insulin delivery. *Int J Pharm* 2013;**455**:259–66.
47. Hosseini-nasab S, Pashaei-Asl R, Khandaghi AA, Nasrabadi HT, Nejati-Koshki K, Akbarzadeh A, et al. Synthesis, characterization, and *in vitro* studies of PLGA-PEG nanoparticles for oral insulin delivery. *Chem Biol Drug Des* 2014;**84**:307–15.
48. Kim SK, Lee S, Jin S, Moon HT, Jeon OC, Lee DY, et al. Diabetes correction in pancreatectomized canines by orally absorbable insulin-deoxycholate complex. *Mol Pharm* 2010;**7**:708–17.
49. Karamanidou T, Karidi K, Bourganis V, Kontonikola K, Kammona O, Kiparissides C. Effective incorporation of insulin in mucus permeating self-nanoemulsifying drug delivery systems. *Eur J Pharm Biopharm* 2015;**97**:223–9.
50. Li X, Guo S, Zhu C, Zhu Q, Gan Y, Rantanen J, et al. Intestinal mucosa permeability following oral insulin delivery using core shell corona nanolipoparticles. *Biomaterials* 2013;**34**:9678–87.
51. Maroni A, Del Curto MD, Salmaso S, Zema L, Melocchi A, Caliceti P, et al. *In vitro* and *in vivo* evaluation of an oral multiple-unit formulation for colonic delivery of insulin. *Eur J Pharm Biopharm* 2016;**108**:76–82.
52. Niu M, Lu Y, Hovgaard L, Guan P, Tan Y, Lian R, et al. Hypoglycemic activity and oral bioavailability of insulin-loaded liposomes containing bile salts in rats: the effect of cholate type, particle size and administered dose. *Eur J Pharm Biopharm* 2012;**81**:265–72.
53. Sharma G, van der Walle CF, Ravi Kumar MN. Antacid co-encapsulated polyester nanoparticles for peroral delivery of insulin: development, pharmacokinetics, biodistribution and pharmacodynamics. *Int J Pharm* 2013;**440**:99–110.
54. Sonaje K, Lin YH, Juang JH, Wey SP, Chen CT, Sung HW. *In vivo* evaluation of safety and efficacy of self-assembled nanoparticles for oral insulin delivery. *Biomaterials* 2009;**30**:2329–39.

55. Zhang X, Qi J, Lu Y, He W, Li X, Wu W. Biotinylated liposomes as potential carriers for the oral delivery of insulin. *Nanomedicine* 2014;**10**:167–76.
56. Abuhelwa AY, Williams DB, Upton RN, Foster DJ. Food, gastrointestinal pH, and models of oral drug absorption. *Eur J Pharm Biopharm* 2017;**112**:234–48.
57. Ensign LM, Cone R, JH. Oral drug delivery with polymeric nanoparticles: the gastrointestinal mucus barriers. *Adv Drug Deliv Rev* 2012;**64**:557–70.
58. Wang X, Sherman A, Liao G, Leong KW, Daniell H, Terhorst C, et al. Mechanism of oral tolerance induction to therapeutic proteins. *Adv Drug Deliv Rev* 2013;**65**:759–73.
59. Yun Y, Cho YW, Park K. Nanoparticles for oral delivery: targeted nanoparticles with peptidic ligands for oral protein delivery. *Adv Drug Deliv Rev* 2013;**65**:822–32.
60. Deep HS, Roychowdhury S, Verma P, Bhandari V. A review on recent advances of enteric coating. *J Pharm* 2012;**2**:5–11.
61. Chuang EY, Lin KJ, Lin PY, Chen HL, Wey SP, Mi FL, et al. Self-assembling bubble carriers for oral protein delivery. *Biomaterials* 2015;**64**:115–24.
62. Renukuntla J, Vadlapudi AD, Patel A, Boddu SHS, Mitra AK. Approaches for enhancing oral bioavailability of peptides and proteins. *Int J Pharm* 2013;**447**:75–93.
63. Grabovac V, Guggi D, Bernkop-Schnurch A. Comparison of the mucoadhesive properties of various polymers. *Adv Drug Deliv Rev* 2005;**57**:1713–23.
64. Griffin BT, Guo J, Presas E, Donovan MD, Alonso MJ, O'Driscoll CM. Pharmacokinetic, pharmacodynamic and biodistribution following oral administration of nanocarriers containing peptide and protein drugs. *Adv Drug Deliv Rev* 2016;**106**:367–80.
65. Czuba E, Diop M, Mura C, Schaschkow A, Langlois A, Bietiger W, et al. Oral insulin delivery, the challenge to increase insulin bioavailability: influence of surface charge in nanoparticle system. *Int J Pharm* 2018;**542**:47–55.
66. Barbari GR, Dorkoosh FA, Amini M, Sharifzadeh M, Atyabi F, Balalaie S, et al. A novel nanoemulsion-based method to produce ultrasmall, water-dispersible nanoparticles from chitosan, surface modified with cell-penetrating peptide for oral delivery of proteins and peptides. *Int J Nanomed* 2017;**12**:3471–83.
67. He Z, Santos JL, Tian H, Huang H, Hu Y, Liu L, et al. Scalable fabrication of size-controlled chitosan nanoparticles for oral delivery of insulin. *Biomaterials* 2017;**130**:28–41.
68. Hinkley GK, Carpinone P, Munson JW, Powers KW, Roberts SM. Oral absorption of PEG-coated versus uncoated gold nanospheres: does agglomeration matter?. *Part Fibre Toxicol* 2015;**12**:9.
69. Choonara BF, Choonara YE, Kumar P, Bijukumar D, du Toit LC, Pillay V. A review of advanced oral drug delivery technologies facilitating the protection and absorption of protein and peptide molecules. *Biotechnol Adv* 2014;**32**:1269–82.
70. Kou L, Sun J, Zhai Y, He Z. The endocytosis and intracellular fate of nanomedicines: implication for rational design. *Asian J Pharm Sci* 2013;**8**:1–10.
71. Rehmani S, Dixon JE. Oral delivery of anti-diabetes therapeutics using cell penetrating and transcytosing peptide strategies. *Peptides* 2018;**100**:24–35.
72. Komin A, Russell LM, Hristova KA, Searson PC. Peptide-based strategies for enhanced cell uptake, transcellular transport, and circulation: mechanisms and challenges. *Adv Drug Deliv Rev* 2017;**110–111**:52–64.
73. Lundquist P, Artursson P. Oral absorption of peptides and nanoparticles across the human intestine: opportunities, limitations and studies in human tissues. *Adv Drug Deliv Rev* 2016;**106**:256–76.
74. Yameen B, Choi WI, Vilos C, Swami A, Shi J, Farokhzad OC. Insight into nanoparticle cellular uptake and intracellular targeting. *J Control Release* 2014;**190**:485–99.
75. Su H, Wang Y, Liu S, Wang Y, Liu Q, Liu G, et al. Emerging transporter-targeted nanoparticulate drug delivery systems. *Acta Pharm Sin B* 2019;**9**:49–58.
76. Bae YH, Lee Y-K, Nurunnabi M, Hee SW, Kwag D. Compositions and methods for bile acid particles. 2016. Available from: ([https://worldwide.espacenet.com/publicationDetails/biblio?DB=EPODOC&II=0&ND=3&adjacent=true&locale=en\\_EP&FT=D&date=20171115&CC=KR&NR=20170125793A&KC=A](https://worldwide.espacenet.com/publicationDetails/biblio?DB=EPODOC&II=0&ND=3&adjacent=true&locale=en_EP&FT=D&date=20171115&CC=KR&NR=20170125793A&KC=A)).
77. Park J, Choi JU, Kim K, Byun Y. Bile acid transporter mediated endocytosis of oral bile acid conjugated nanocomplex. *Biomaterials* 2017;**147**:145–54.
78. Fan W, Xia D, Zhu Q, Li X, He S, Zhu C, et al. Functional nanoparticles exploit the bile acid pathway to overcome multiple barriers of the intestinal epithelium for oral insulin delivery. *Biomaterials* 2018;**151**:13–23.
79. Samstein RM, Perica K, Balderrama F, Look M, Fahmy TM. The use of deoxycholic acid to enhance the oral bioavailability of biodegradable nanoparticles. *Biomaterials* 2008;**29**:703–8.
80. Niu M, Lu Y, Hovgaard L, Wu W. Liposomes containing glycocholate as potential oral insulin delivery systems: preparation, *in vitro* characterization, and improved protection against enzymatic degradation. *Int J Nanomed* 2011;**6**:1155–66.
81. Niu M, Tan Y, Guan P, Hovgaard L, Lu Y, Qi J, et al. Enhanced oral absorption of insulin-loaded liposomes containing bile salts: a mechanistic study. *Int J Pharm* 2014;**460**:119–30.
82. Omid JN, Javan NB, Dehpour AR, Partoazar A, Tehrani MR, Dorkoosh F. *In-vitro* and *in-vivo* cytotoxicity and efficacy evaluation of novel glycyl-glycine and alanyl-alanine conjugates of chitosan and trimethyl chitosan nano-particles as carriers for oral insulin delivery. *Int J Pharm* 2018;**535**:293–307.
83. Li L, Jiang G, Yu W, Liu D, Chen H, Liu Y, et al. Preparation of chitosan-based multifunctional nanocarriers overcoming multiple barriers for oral delivery of insulin. *Mater Sci Eng C Mater Biol Appl* 2017;**70**:278–86.
84. Zhang P, Xu Y, Zhu X, Huang Y. Goblet cell targeting nanoparticle containing drug-loaded micelle cores for oral delivery of insulin. *Int J Pharm* 2015;**496**:993–1005.
85. Lee JH, Sahu A, Choi WI, Lee JY, Tae G. ZOT-derived peptide and chitosan functionalized nanocarrier for oral delivery of protein drug. *Biomaterials* 2016;**103**:160–9.
86. Wu L, Liu M, Shan W, Zhu X, Li L, Zhang Z, et al. Bioinspired butyrate-functionalized nanovehicles for targeted oral delivery of biomacromolecular drugs. *J Control Release* 2017;**262**:273–83.
87. Cho HJ, Oh J, Choo MK, Ha JJ, Park Y, Maeng HJ. Chondroitin sulfate-capped gold nanoparticles for the oral delivery of insulin. *Int J Biol Macromol* 2014;**63**:15–20.
88. Salvioni L, Fiandra L, Del Curto MD, Mazzucchelli S, Allevi R, Truffi M, et al. Oral delivery of insulin via polyethylene imine-based nanoparticles for colonic release allows glycemic control in diabetic rats. *Pharmacol Res* 2016;**110**:122–30.
89. Niu Z, Conejos-Sanchez I, Griffin BT, O'Driscoll CM, Alonso MJ. Lipid-based nanocarriers for oral peptide delivery. *Adv Drug Deliv Rev* 2016;**106**:337–54.
90. Kalepun S, Manthina M, Veerabhadhraswamy P. Oral lipid-based drug delivery systems—an overview. *Acta Pharm Sin B* 2013;**3**:361–72.
91. Nguyen TX, Huang L, Gauthier M, Yang G, Wang W. Recent advances in liposome surface modification for oral drug delivery. *Nanomedicine* 2016;**11**:1169–85.
92. Cui M, Wu W, Hovgaard L, Lu Y, Chen D, Qi J. Liposomes containing cholesterol analogues of botanical origin as drug delivery systems to enhance the oral absorption of insulin. *Int J Pharm* 2015;**489**:277–84.
93. Leitner VM, Marschutz MK, Bernkop-Schnurch A. Mucoadhesive and cohesive properties of poly(acrylic acid) cysteine conjugates with regard to their molecular mass. *Eur J Pharm Sci* 2003;**18**:89–96.
94. Schnürch AB, Kast CE, Guggi D. Permeation enhancing polymers in oral delivery of hydrophilic macromolecules: thiomers/gsh systems. *J Control Release* 2003;**93**:95–103.
95. Werle M, Hoffer M. Glutathione and thiolated chitosan inhibit multidrug resistance P-glycoprotein activity in excised small intestine. *J Control Release* 2006;**111**:41–6.

96. Jacobsen AC, Jensen SM, Fricker G, Brandl M, Treusch AH. Archaeal lipids in oral delivery of therapeutic peptides. *Eur J Pharm Sci* 2017;**108**:101–10.
97. Parmentier J, Becker MM, Heintz U, Fricker G. Stability of liposomes containing bio-enhancers and tetraether lipids in simulated gastro-intestinal fluids. *Int J Pharm* 2011;**405**:210–7.
98. Sharma S, Jyoti K, Sinha R, Katyal A, Jain UK, Madan J. Protamine coated proliposomes of recombinant human insulin encased in Eudragit S100 coated capsule offered improved peptide delivery and permeation across Caco-2 cells. *Mater Sci Eng C Mater Biol Appl* 2016;**67**:378–85.
99. Li D, Zhuang J, Yang Y, Wang D, Yang J, He H, et al. Loss of integrity of doxorubicin liposomes during transcellular transportation evidenced by fluorescence resonance energy transfer effect. *Colloids Surf B Biointerfaces* 2018;**171**:224–32.
100. Roger E, Gimel JC, Bensley C, Klymchenko AS, Benoit JP. Lipid nanocapsules maintain full integrity after crossing a human intestinal epithelium model. *J Control Release* 2017;**253**:11–8.
101. Wang T, Xue J, Hu Q, Zhou M, Luo Y. Preparation of lipid nanoparticles with high loading capacity and exceptional gastro-intestinal stability for potential oral delivery applications. *J Colloid Interface Sci* 2017;**507**:119–30.
102. Hecq J, Amighi K, Goole J. Development and evaluation of insulin-loaded cationic solid lipid nanoparticles for oral delivery. *J Drug Deliv Sci Technol* 2016;**36**:192–200.
103. Boushra M, Tous S, Fetih G, Korzekwa K, Lebo DB, Xue HY, et al. Development and evaluation of viscosity-enhanced nanocarrier (VEN) for oral insulin delivery. *Int J Pharm* 2016;**511**:462–72.
104. Yuan H, Chen C-Y, Chai G-h, Du Y-Z, Hu F-Q. Improved transport and absorption through gastrointestinal tract by pegylated solid lipid nanoparticles. *Mol Pharm* 2013;**10**:1865–73.
105. Friedl H, Dunnhaupt S, Hintzen F, Waldner C, Parikh S, Pearson JP, et al. Development and evaluation of a novel mucus diffusion test system approved by self-nanoemulsifying drug delivery systems. *J Pharm Sci* 2013;**102**:4406–13.
106. Li P, Tan A, Prestidge CA, Nielsen HM, Mullertz A. Self-nanoemulsifying drug delivery systems for oral insulin delivery: *in vitro* and *in vivo* evaluations of enteric coating and drug loading. *Int J Pharm* 2014;**477**:390–8.
107. Griesser J, Hetényi G, Kadas H, Demarne F, Jannin V, Bernkop-Schnürch A. Self-emulsifying peptide drug delivery systems: how to make them highly mucus permeating. *Int J Pharm* 2018;**538**:159–66.
108. Hetényi G, Griesser J, Moser M, Demarne F, Jannin V, Bernkop-Schnürch A. Comparison of the protective effect of self-emulsifying peptide drug delivery systems towards intestinal proteases and glutathione. *Int J Pharm* 2017;**523**:357–65.
109. Iqbal M, Zafar N, Fessi H, Elaissari A. Double emulsion solvent evaporation techniques used for drug encapsulation. *Int J Pharm* 2015;**496**:173–90.
110. Dogru ST, Calis S, Oner F. Oral multiple w/o/w emulsion formulation of a peptide salmon calcitonin: *in vitro*–*in vivo* evaluation. *J Clin Pharm Thera* 2000;**25**:435–43.
111. Venkata ST, Senthil V, Sai KI, Basha KR, Madhunapantula VS. Design and development of oral nanoparticulated insulin in multiple emulsion. *Curr Drug Deliv* 2014;**11**:472–85.
112. Griffin BT, O'Driscoll CM. Design of lipid nanoparticles for the oral delivery of hydrophilic macromolecules. *Colloids Surf B Biointerfaces* 2002;**27**:159–68.
113. Li X, Qi J, Xie Y, Zhang X, Hu S, Xu Y, et al. Nanoemulsions coated with alginate/chitosan as oral insulin delivery systems: preparation, characterization, and hypoglycemic effect in rats. *Int J Nanomed* 2013;**8**:23–32.
114. Agrawal GR, Wakte P, Shelke S. Formulation, physicochemical characterization and *in vitro* evaluation of human insulin-loaded microspheres as potential oral carrier. *Prog Biomater* 2017;**6**:125–36.
115. Liu Z, Jiao Y, Wang Y, Zhou C, Zhang Z. Polysaccharides-based nanoparticles as drug delivery systems. *Adv Drug Deliv Rev* 2008;**60**:1650–62.
116. Su FY, Lin KJ, Sonaje K, Wey SP, Yen TC, Ho YC, et al. Protease inhibition and absorption enhancement by functional nanoparticles for effective oral insulin delivery. *Biomaterials* 2012;**33**:2801–11.
117. Chuang EY, Lin KJ, Su FY, Chen HL, Maiti B, Ho YC, et al. Calcium depletion-mediated protease inhibition and apical-junctional-complex disassembly via an EGTA-conjugated carrier for oral insulin delivery. *J Control Release* 2013;**169**:296–305.
118. Chuang EY, Nguyen GT, Su FY, Lin KJ, Chen CT, Mi FL, et al. Combination therapy via oral co-administration of insulin- and exendin-4-loaded nanoparticles to treat type 2 diabetic rats undergoing OGTT. *Biomaterials* 2013;**34**:7994–8001.
119. Wong CY, Al-Salami H, Dass CR. The role of chitosan on oral delivery of peptide-loaded nanoparticle formulation. *J Drug Target* 2018;**26**:551–62.
120. Wang J, Xu M, Cheng X, Kong M, Liu Y, Feng C, et al. Positive/negative surface charge of chitosan based nanogels and its potential influence on oral insulin delivery. *Carbohydr Polym* 2016;**136**:867–74.
121. Sheng J, He H, Han L, Qin J, Chen S, Ru G, et al. Enhancing insulin oral absorption by using mucoadhesive nanoparticles loaded with LMWP-linked insulin conjugates. *J Control Release* 2016;**233**:181–90.
122. Li L, Yang L, Li M, Zhang L. A cell-penetrating peptide mediated chitosan nanocarriers for improving intestinal insulin delivery. *Carbohydr Polym* 2017;**174**:182–9.
123. Balakrishnan A, Polli JE. Apical sodium dependent bile acid transporter (ASBT, SLC10A2): a potential prodrug target. *Mol Pharm* 2006;**3**:223–30.
124. Al-Hilal TA, Chung SW, Alam F, Park J, Lee KE, Jeon H, et al. Functional transformations of bile acid transporters induced by high-affinity macromolecules. *Sci Rep* 2014;**4**:4163.
125. Nurunnabi M, Khatun Z, Revuri V, Nafujjaman M, Cha S, Cho S, et al. Design and strategies for bile acid mediated therapy and imaging. *RSC Adv* 2016;**6**:73986–4002.
126. Champcion JA, Walker A, Mitragotri S. Role of particle size in phagocytosis of polymeric microspheres. *Pharm Res* 2008;**25**:1815–21.
127. Sarmiento B, Mazzaglia D, Bonferoni MC, Neto AP, do Céu Monteiro M, Seabra V. Effect of chitosan coating in overcoming the phagocytosis of insulin loaded solid lipid nanoparticles by mononuclear phagocyte system. *Carbohydr Polym* 2011;**84**:919–25.
128. Xu B, Jiang G, Yu W, Liu D, Liu Y, Kong X, et al. Preparation of poly(lactic-co-glycolic acid) and chitosan composite nanocarriers via electrostatic self assembly for oral delivery of insulin. *Mater Sci Eng C Mater Biol Appl* 2017;**78**:420–8.
129. Millotti G, Laffleur F, Perera G, Vigl C, Pickl K, Sinner F, et al. *In vivo* evaluation of thiolated chitosan tablets for oral insulin delivery. *J Pharm Sci* 2014;**103**:3165–70.
130. Kast CE, Bernkop-Schnürch A. Thiolated polymers–thiomers: development and *in vitro* evaluation of chitosan–thioglycolic acid conjugates. *Biomaterials* 2001;**22**:2345–52.
131. Liu M, Zhang J, Zhu X, Shan W, Li L, Zhong J, et al. Efficient mucus permeation and tight junction opening by dissociable "mucus-inert" agent coated trimethyl chitosan nanoparticles for oral insulin delivery. *J Control Release* 2016;**222**:67–77.
132. Bader RA, Wardwell PR. Polysialic acid: overcoming the hurdles of drug delivery. *Ther Deliv* 2014;**5**:235–7.
133. Zhang T, She Z, Huang Z, Li J, Luo X, Deng Y. Application of sialic acid/polysialic acid in the drug delivery systems. *Asian J Pharm Sci* 2014;**9**:75–81.
134. Wu J, Lu S, Zheng Z, Zhu L, Zhan X. Modification with polysialic acid-PEG copolymer as a new method for improving the therapeutic efficacy of proteins. *Prep Biochem Biotechnol* 2016;**46**:788–97.
135. Thwala LN, Belouqui A, Csaba NS, Gonzalez-Touceda D, Tovar S, Dieguez C, et al. The interaction of protamine nanocapsules with the intestinal epithelium: a mechanistic approach. *J Control Release* 2016;**243**:109–20.
136. Mukhopadhyay P, Chakraborty S, Bhattacharya S, Mishra R, Kundu PP. pH-sensitive chitosan/alginate core-shell nanoparticles for efficient and safe oral insulin delivery. *Int J Biol Macromol* 2015;**72**:640–8.

137. Zhang X, Cheng H, Dong W, Zhang M, Liu Q, Wang X, et al. Design and intestinal mucus penetration mechanism of core-shell nanocomplex. *J Control Release* 2018;**272**:29–38.
138. Lopes M, Shrestha N, Correia A, Shahbazi MA, Sarmiento B, Hirvonen J, et al. Dual chitosan/albumin-coated alginate/dextran sulfate nanoparticles for enhanced oral delivery of insulin. *J Control Release* 2016;**232**:29–41.
139. Song Y, Gan W, Li Q, Guo Y, Zhou J, Zhang L. Alkaline hydrolysis and flocculation properties of acrylamide-modified cellulose polyelectrolytes. *Carbohydr Polym* 2011;**86**:171–6.
140. Makhlof A, Tozuka Y, Takeuchi H. Design and evaluation of novel pH-sensitive chitosan nanoparticles for oral insulin delivery. *Eur J Pharm Sci* 2011;**42**:445–51.
141. Singh B, Maharjan S, Jiang T, Kang SK, Choi YJ, Cho CS. Attuning hydroxypropyl methylcellulose phthalate to oral delivery vehicle for effective and selective delivery of protein vaccine in ileum. *Biomaterials* 2015;**59**:144–59.
142. Wu ZM, Zhou L, Guo XD, Jiang W, Ling L, Qian Y, et al. HP55-coated capsule containing PLGA/RS nanoparticles for oral delivery of insulin. *Int J Pharm* 2012;**425**:1–8.
143. Wang Y, Chen BZ, Liu YJ, Wu ZM, Guo XD. Application of mesoscale simulation to explore the aggregate morphology of pH-sensitive nanoparticles used as the oral drug delivery carriers under different conditions. *Colloids Surf B Biointerfaces* 2017;**151**:280–6.
144. Mukhopadhyay P, Sarkar K, Bhattacharya S, Bhattacharyya A, Mishra R, Kundu PP. pH sensitive *N*-succinyl chitosan grafted polyacrylamide hydrogel for oral insulin delivery. *Carbohydr Polym* 2014;**112**:627–37.
145. Mo R, Jiang T, Di J, Tai W, Gu Z. Emerging micro- and nanotechnology based synthetic approaches for insulin delivery. *Chem Soc Rev* 2014;**43**:3595–629.
146. Amirthalingam E, Rodrigues M, Casal-Dujat L, Calpena AC, Amabilino DB, Ramos-Lopez D, et al. Macrocyclic imidazolium-based amphiphiles for the synthesis of gold nanoparticles and delivery of anionic drugs. *J Colloid Interface Sci* 2015;**437**:132–9.
147. Sant S, Tao SL, Fisher OZ, Xu Q, Peppas NA, Khademhosseini A. Microfabrication technologies for oral drug delivery. *Adv Drug Del Rev* 2012;**64**:496–507.
148. Hu L, Sun H, Zhao Q, Han N, Bai L, Wang Y, et al. Multilayer encapsulated mesoporous silica nanospheres as an oral sustained drug delivery system for the poorly water-soluble drug felodipine. *Mater Sci Eng C Mater Biol Appl* 2015;**47**:313–24.
149. Kapoor S, Hegde R, Bhattacharyya AJ. Influence of surface chemistry of mesoporous alumina with wide pore distribution on controlled drug release. *J Control Release* 2009;**140**:34–9.
150. Kamari Y, Ghiaci P, Ghiaci M. Study on montmorillonite/insulin/TiO<sub>2</sub> hybrid nanocomposite as a new oral drug-delivery system. *Mater Sci Eng C Mater Biol Appl* 2017;**75**:822–8.
151. Diaz A, David A, Perez R, Gonzalez ML, Baez A, Wark SE, et al. Nanoencapsulation of insulin into zirconium phosphate for oral delivery applications. *Biomacromol* 2010;**11**:2465–70.
152. Deng W, Xie Q, Wang H, Ma Z, Wu B, Zhang X. Selenium nanoparticles as versatile carriers for oral delivery of insulin: insight into the synergic antidiabetic effect and mechanism. *Nanomedicine* 2017;**13**:1965–74.
153. Zhang Y, Zhang L, Ban Q, Li J, Li CH, Guan YQ. Preparation and characterization of hydroxyapatite nanoparticles carrying insulin and gallic acid for insulin oral delivery. *Nanomedicine* 2018;**14**:353–64.
154. Hoffmann F, Cornelius M, Morell J, Froba M. Silica-based mesoporous organic-inorganic hybrid materials. *Angew Chem Int Ed Engl* 2006;**45**:3216–51.
155. Westcott SL, Oldenburg SJ, Lee TR, Halas NJ. Formation and adsorption of clusters of gold nanoparticles onto functionalized silica nanoparticle surfaces. *Langmuir* 1998;**14**:5396–401.
156. Zhao X, Shan C, Zu Y, Zhang Y, Wang W, Wang K, et al. Preparation, characterization, and evaluation *in vivo* of Ins-SiO<sub>2</sub>-HP55 (insulin-loaded silica coating HP55) for oral delivery of insulin. *Int J Pharm* 2013;**454**:278–84.
157. Andreani T, Miziara L, Lorenzon EN, de Souza AL, Kiill CP, Fangueiro JF, et al. Effect of mucoadhesive polymers on the *in vitro* performance of insulin-loaded silica nanoparticles: interactions with mucin and biomembrane models. *Eur J Pharm Biopharm* 2015;**93**:118–26.
158. Mohanraj VJ, Barnes TJ, Prestidge CA. Silica nanoparticle coated liposomes: a new type of hybrid nanocapsule for proteins. *Int J Pharm* 2010;**392**:285–93.
159. Safari M, Kamari Y, Ghiaci M, Sadeghi-Aliabadi H, Mirian M. Synthesis and characterization of insulin/zirconium phosphate@TiO<sub>2</sub> hybrid composites for enhanced oral insulin delivery applications. *Drug Dev Ind Pharm* 2017;**43**:862–70.
160. Fonte P, Araujo F, Silva C, Pereira C, Reis S, Santos HA, et al. Polymer-based nanoparticles for oral insulin delivery: revisited approaches. *Biotechnol Adv* 2015;**33**:1342–54.
161. Inchaurrega L, Martin-Arbella N, Zabaleta V, Quincoces G, Penuelas I, Irache JM. *In vivo* study of the mucus-permeating properties of PEG-coated nanoparticles following oral administration. *Eur J Pharm Biopharm* 2015;**97**:280–9.
162. He H, Ye J, Liu E, Liang Q, Liu Q, Yang VC. Low molecular weight protamine (LMWP): a nontoxic protamine substitute and an effective cell-penetrating peptide. *J Control Release* 2014;**193**:63–73.
163. Shan W, Zhu X, Liu M, Li L, Zhong J, Sun W, et al. Overcoming the diffusion barrier of mucus and absorption barrier of epithelium by self-assembled nanoparticles for oral delivery of insulin. *ACS Nano* 2015;**9**:2345–56.
164. Garcia-Diaz M, Foged C, Nielsen HM. Improved insulin loading in poly(lactic-co-glycolic) acid (PLGA) nanoparticles upon self-assembly with lipids. *Int J Pharm* 2015;**482**:84–91.
165. Müller C, Perera G, König V, Bernkop-Schnurch A. Development and *in vivo* evaluation of papain-functionalized nanoparticles. *Eur J Pharm Biopharm* 2014;**87**:125–31.
166. Pereira de Sousa I, Cattoz B, Wilcox MD, Griffiths PC, Dalglish R, Rogers S, et al. Nanoparticles decorated with proteolytic enzymes, a promising strategy to overcome the mucus barrier. *Eur J Pharm Biopharm* 2015;**97**:257–64.
167. Sharma R, Gupta U, Garg NK, Tyagi RK, Jain NK. Surface engineered and ligand anchored nanobioconjugate: an effective therapeutic approach for oral insulin delivery in experimental diabetic rats. *Colloids Surf B Biointerfaces* 2015;**127**:172–81.
168. Niu Z, Samaridou E, Jaumain E, Coene J, Ullio G, Shrestha N, et al. PEG-PGA enveloped octaarginine-peptide nanocomplexes: an oral peptide delivery strategy. *J Control Release* 2018;**276**:125–39.
169. Harloff-Helleberg S, Nielsen LH, Nielsen HM. Animal models for evaluation of oral delivery of biopharmaceuticals. *J Control Release* 2017;**268**:57–71.
170. Yu M, Yang Y, Zhu C, Guo S, Gan Y. Advances in the transepithelial transport of nanoparticles. *Drug Discov Today* 2016;**21**:1155–61.
171. Fan W, Xia D, Zhu Q, Hu L, Gan Y. Intracellular transport of nanocarriers across the intestinal epithelium. *Drug Discov Today* 2016;**21**:856–63.